The virome from a collection of endomycorrhizal fungi reveals new viral taxa with unprecedented genome organization

Suvi Sutela, Marco Forgia, Eeva J Vainio, Marco Chiapello, Stefania Daghino, Marta Vallino, Elena Martino, Mariangela Girlanda, Silvia Perotto, Massimo Turina

The virome from a collection of endomycorrhizal fungi reveals new viral taxa with unprecedented genome organization

Suvi Sutela[1*], Marco Forgia[2*], Eeva J. Vainio[1], Marco Chiapello[2], Stefania Daghino[3], Marta Vallino[2], Elena Martino[3], Mariangela Girlanda[3], Silvia Perotto[3], Massimo Turina[2]

[1] Natural Resources Institute Finland (Luke), Forest Health and Biodiversity Group, Latokartanonkaari 9, FI-00790 Helsinki, FINLAND
[2] Institute for Sustainable Plant Protection, CNR, Strada delle Cacce 73, 10135 Torino, ITALY
[3] Department of Life Science and Systems Biology, University of Torino, Viale Mattioli 25, 10125 Torino, ITALY

*First and second author contributed equally to the manuscript

Corresponding Author information
Massimo Turina, **Email:** massimo.turina@ipsp.cnr.it
Institute for Sustainable Plant Protection
CNR- Strada delle Cacce 73
10135 Torino, ITALY

Suvi Sutela, https://orcid.org/0000-0003-0426-0718; Marco Forgia, https://orcid.org/0000-0003-0101-1046; Eeva J. Vainio, https://orcid.org/0000-0002-6739-7968; Marco Chiapello, https://orcid.org /0000-0001-7768-3047; Stefania Daghino, https://orcid.org /0000-0001-5722-1558; Elena Martino, https://orcid.org/0000-0003-3446-2994; Mariangela Girlanda, https://orcid.org/0000-0003-0332-9103; Silvia Perotto, https://orcid.org/0000-0003-0121-1806; Massimo Turina, https://orcid.org/0000-0002-9659-9470.

Keywords
Viruses, ericoid mycorrhizal fungi, orchid mycorrhizal fungi, RNA-dependent RNA polymerase

Author Contributions
E.J.V., S.S, S.P., and M.T. designed research; M.C., M.F., S.S., M.T., and M.V. performed research and analyzed data; S.D., M.G., E.M., and S.P. provided resources; E.J.V., S.D., S.P. conducted review and editing; S.P., M.T., and E.J.V. provided funding acquisition and project administration; and M.F., S.D., S.P., S.S., and M.T. wrote the paper.

This PDF file includes:
Main Text
Figures 1 to 7
Tables 1 to 2

Abstract

Mutualistic plant-associated fungi are recognized as important drivers in plant evolution, diversity and health. The discovery that mycoviruses can take part and play important roles in symbiotic tripartite interactions has prompted us to study the viromes associated with a collection of ericoid and orchid mycorrhizal (ERM and ORM, respectively) fungi. Our study, based on high-throughput sequencing of transcriptomes (RNAseq) from fungal isolates grown in axenic cultures, revealed in both ERM and ORM fungi the presence of new mycoviruses closely related to already classified virus taxa, but also new viruses that expand the boundaries of characterized RNA virus diversity to previously undescribed evolutionary trajectories. In ERM fungi, we provide first evidence of a bipartite virus, distantly related to narnaviruses, that splits the RNA-dependent RNA polymerase (RdRP) palm domain into two distinct proteins, encoded by each of the two segments. Furthermore, in one isolate of the ORM fungus *Tulasnella* spp. we detected a 12 kb genomic fragment coding for an RdRP with features of bunyavirus-like RdRPs. However, this 12 kb genomic RNA has the unique features, for *Bunyavirales* members, of being tri-cistronic and carrying ORFs for the putative RdRP and putative nucleocapsid in ambisense orientation on the same genomic RNA. Finally, a number of ORM fungal isolates harbored a group of ambisense bicistronic viruses with a genomic size of around 5 kb, where we could identify a putative RdRP palm domain that has some features of plus strand RNA viruses; these new viruses may represent a new lineage in the Riboviria, as they could not be reliably assigned to any of the branches in the recently derived monophyletic tree that includes most viruses with an RNA genome.

1. Introduction

Viruses affect our lives in pervasive ways, as proved by the current SARS-CoV-2-caused pandemic (Wu et al. 2020) and, up to a decade ago, knowledge of virus biodiversity—the virosphere—was strongly biased by focus on viruses that affect our health, or that cause economic damage by infecting our plant crops, or the animals we have domesticated. Such anthropocentric view of viruses as the ultimate pathogens neglects their basic influence in the evolution of life as we know it (Ryan 2009), or their immense effects on ecological systems as controller of microbial populations (Rohwer et al. 2009), particularly in the oceans (Suttle 2007). Describing viral diversity and the evolutionary relationships among viruses is not a mere classificatory exercise, but it has profound impacts, for example to elucidate their origins and the origin of life (Krupovic et al. 2019; Krupovic et al. 2020). In practice, virome studies may be used to identify host reservoirs involved in viral spillovers to new species, mostly among vertebrates (Mollentze & Streicker 2020), or to help assess the risk of using specific viruses as biological tools with respect to their host specificity or off-target effects. Our knowledge of the virosphere changed enormously with the contribution of high throughput sequencing (HTS) techniques to characterize viromes associated with different hosts and metagenomic samples in an unbiased approach, independently of their pathogenic potential.

All the viruses with an RNA genome so far characterized share a viral polymerase protein carrying a common domain, called palm domain, at the core of the polymerase catalytic activity (te Velthuis 2014). This domain is shared by both reverse transcriptases and the RNA-dependent RNA polymerases (RdRP); the latter are proteins that amplify viral genomes synthesizing plus and minus stranded RNA from an RNA template. There is now a consensus that known viruses with RNA genomes are monophyletic, and this resulted in a recent effort to reconstruct their evolutionary trajectory in a single phylogenetic tree (Wolf et al. 2018) recognized by the International Committee on Taxonomy of Viruses (ICTV), which currently includes all viruses with an RNA genome in the realm *Riboviria*, and in particular those that use an RdRP for their replication are placed in the kingdom *Orthornavirae* (Koonin et al. 2020). The greater contribution to the characterization of the diversity of the RNA virosphere comes from studies on the viromes of invertebrates, mainly from arthropods (Li et al. 2015; Shi et al. 2016; Kaefer et al. 2019). The same HTS techniques have been applied to the characterization of viromes associated with fungi, but the number of fungal hosts investigated is still very low (Vainio et al. 2015; Marzano et al. 2016; Donaire & Ayllon 2017; Nerva et al. 2019a) and their contribution to the overall diversity of fungal viruses (mycoviruses) is limited. A more traditional approach based on the characterization of individual viruses has nevertheless allowed the identification of new classes of mycoviruses, such as the first negative strand mycovirus (Liu et al. 2014), the first ssDNA mycovirus (Yu et al. 2010) or new polysegmented RNA mycoviruses with limited resemblance to existing RNA viruses (Kanhayuwa et al. 2015; Sato et al. 2020).

Mycoviruses were discovered in the early 1960's as a cause of disease in the cultivated mushroom *Agaricus bisporus* (Hollings 1962) and were later found in most fungal taxa investigated (Ghabrial et al. 2015). Although fungi occupy virtually all ecological niches, mycoviruses of plant-interacting fungi are particularly significant for crop protection because they can influence the phenotype of their host. In particular, mycoviruses that cause hypovirulence in phytopathogenic fungi have attracted a lot of interest over the last few decades for their possible use as biocontrol agents (Pearson et al. 2009). In addition, fungi that interact with plants are of

particular interest as recent studies have shown that, in virus-fungus-plant tripartite interactions, mycoviruses could spread beyond their native fungal hosts and be transferred to host plants by horizontal virus transfers (HVTs); similarly, plant viruses can be transferred to plant-interacting fungi. Indirect evidence of such HVTs derives from phylogenetic analysis of some RNA virus clades, which include closely related plant viruses and mycoviruses, as is the case for the *Partitiviridae*, the *Endornaviridae* and the *Mitoviridae*, suggesting a relatively recent cross-kingdom virus transmission (Roossinck 2019). Such HVTs often resulted in cryptic persistent viral plant infections that might provide specific beneficial traits (Takahashi et al. 2019). Evidence of cross-kingdom HVT was indeed shown for plant viruses replicating in fungi both experimentally (Mascia et al. 2019) and naturally (Andika et al. 2017), and for mycoviruses replicating in plant cells (Nerva et al. 2017) and in whole plants (Bian et al. 2020).

So far, most studies on mycoviruses of plant-interacting fungi have focused on phytopathogenic fungi as model systems, but other biological systems could have an even greater significance to investigate the interplay among mycoviruses, fungi and plant hosts. In addition to fungal pathogens, plants interact in fact with a broad spectrum of fungal endophytes that reside within the plant tissues as symbionts, often contributing to plant growth and/or defense against biotic and abiotic stress (Gange et al. 2019). Based on their life histories, taxonomic position and colonized host plants/organs, fungal endophytes have been classified into four groups (Rodriguez et al. 2009), and mycoviruses have been found in all four groups (Herrero et al. 2009; Bao & Roossinck 2013). Another taxonomically heterogenous group of fungi in close relationship with plants are the mycorrhizal fungi, which differ from endophytes because they form recognizable fungal inter- or intracellular structures within the root tissues. In ectomycorrhizas, mainly formed by basidiomycetes and some ascomycetes, the fungal partner remains confined in the intercellular spaces of the host root tissues. In endomycorrhizas, by contrast, the symbiotic fungal hyphae colonize the root cells and form specialized intracellular plant-fungus interfaces that increase bidirectional exchanges between partners (Bonfante and Genre 2010). Fungi in the subphylum Glomeromycotina form highly branched fungal structures called arbuscules in the majority of angiosperms, giving rise to the arbuscular mycorrhiza, whereas distinct lineages of asco- and basidiomycetes form coiled hyphal structures in specific families of angiosperms, namely the Ericaceae and the Orchidaceae, giving rise to the ericoid mycorrhiza (ERM) and the orchid mycorrhiza (ORM), respectively. ERM fungi are mainly ascomycetes belonging to the class Leotiomycetes, but include some basidiomycetes in the Serendipitaceae family as well (Weiss et al. 2016). ERM fungi interact with the host plant but can also grow as saprotrophs in the soil, where they can degrade a wide range of organic substrates (Smith & Read 2008), thus contributing to the mobilization of nutrients (Read & Stribley 1973) and to the ecological success of their host plants (Smith & Read 2008).

ORM fungi are essential for orchid propagation in nature, since orchids produce minute seeds lacking stored energy sources, which are unable to germinate and develop further unless they are colonized by symbiotic fungi that provide the host with nutrients, including organic carbon. Orchids are usually found to associate with fungi of three families in the Basidiomycota, namely the Tulasnellaceae and Ceratobasidiaceae (Cantharellales) and the Serendipitaceae (Sebacinales) (Dearnaley et al. 2012). These families were previously assigned to the form-genus *Rhizoctonia*.

Mycorrhizal fungi, which contribute profoundly to the growth and health of plant partners, have established a long co-evolution with the roots of most terrestrial plants (Smith & Read 2008). However, mycoviruses have been reported in less than twenty mycorrhizal fungal genera so far, not even covering all different mycorrhizal types (Blattný & Králík 1968; Dieleman-Van Zaayen et

al. 1970; Huttinga et al. 1975; Bai et al. 1997; Stielow and Menzel 2010; Petrzik et al. 2016; Vainio et al. 2017). In particular, no mycoviruses have been reported from ERM fungi so far, and a few mycoviruses have been characterized in ORM fungi from Australia, including a newly described hypovirus and a mitovirus that could not be ascribed to known taxa of the same genera (Ong et al. 2016; Ong et al. 2017; Ong et al. 2018).

To investigate the possible contribution of mycoviruses to the evolution of viruses, we need to increase our knowledge on the diversity and distribution of mycoviruses in mycorrhizal fungi, which have been poorly investigated compared with other fungal groups. The purpose of this work was to characterize the virome of ERM and ORM fungi, involved in two fairly neglected endomycorrhizal types. Endomycorrhizal fungi are particularly interesting fungal hosts to investigate HVT between fungi and plants, and vice-versa, because they maintain close contacts without the onset of structural and molecular host defense, that often can hamper the exchanges in pathogenic plant-fungal interactions. We examined 37 ERM fungal strains, mostly *Oidiodendron maius* isolated from *Vaccinium* species or from *Calluna vulgaris,* and 12 ORM fungal strains in the genera *Tulasnella* and *Ceratobasidium*, isolated from the roots of Mediterranean terrestrial orchids in Italy. The analysis revealed new viral taxa with unprecedented genome organizations, expanding our view of mycovirus diversity, genome structures and phylogenesis of RNA viruses.

2. Materials and Methods

2.1 Origin of the fungal isolates

The ERM and ORM fungi investigated in this study are listed in Supplementary online Table S1. The 37 ERM fungal strains have been previously isolated from roots of *C. vulgaris*, *V. myrtillus*, *V. corymbosum* or *V. angustifolium*, collected in different countries (Italy, Great Britain, Poland, Canada). Two sampling sites were characterized by either mildly (Vallino et al. 2011) or strongly (Martino et al. 2000; Martino et al. 2003) polluted soils. The 12 ORM fungal strains were isolated in Italy, mainly from two terrestrial meadow orchid species: *Serapias vomeracea* and *Orchis purpurea*. Further characteristics of the sites and the isolation and identification methods have been described previously (see references in Supplementary online Table S1). Morphological identification of the strains was confirmed by the sequencing of the ITS regions, available in public databases.

The *R. ericae* (UAMH7375-ICMP18553) and *O. maius* (MUT1381-ATCC MYA-4765) (Martino et al. 2018) genomes are available (Mycocosm Sequencing Project, JGI, USA).

2.2 Fungal RNA extraction

For the extraction of total RNA, fungal strains were cultivated in liquid cultures: ERM strains in Czapek mineral medium (pH 5.6) with 2% glucose (Martino et al. 2000) supplemented with MES (3.9 g l^{-1}); ORM fungal strains in 2% malt extract medium. Fungal cultures were kept on an orbital shaker (~100 rpm) at 24 °C in the dark for three to seven days depending on the growth of the strain. Three ERM fungal strains (MUT1371, MUT2998 and MUT3000) were grown on Czapek-glucose 2% plates covered with cellophane membranes at 24 °C. Mycelia was collected by vacuum filtering through Miracloth, dried and subsequently frozen and stored at -80 °C prior freeze drying of 48 h. RNA extraction was conducted from 15–37 mg of freeze-dried fungal mycelia using the Spectrum Plant Total RNA Kit (Sigma-Aldrich). Briefly, lyophilized fungal mycelia were homogenized in 900 µl of lysis solution with ceramic and glass beads in

FastPrep24. Homogenization (6.5 m/s 30 sec) was conducted three times and the sample mixture was frozen prior to the final homogenization step. Samples were then centrifuged at maximum speed for 5 min at +4 ˚C and approximately 700 µl of the solution was transferred to a new tube and re-centrifuged. Supernatant was transferred to a filtration column and RNA isolation was performed following manufacturer's instructions with the following exceptions: the used binding solution volume was 1:1 to the sample volume, the volume of wash solution 1 and 2 was 700 µl and elution of RNA was conducted with 45 µl of elution solution. RNA quantity and quality were determined using NanoDrop 2000 (Thermo Scientific) and the integrity of ribosomal RNA was confirmed by running an aliquot of RNA on an agarose gel.

2.3 Library construction and assembly and identification of virus-like sequences

Pooled total RNA samples representing 0.5 µg for each fungal strain were sent to Macrogen Korea precipitated in ethanol. The RIN values of pooled RNAs varied between 8.1 and 8.7 and the ribosomal RNA (rRNA) ratios 1.1-1.8. TruSeq Stranded Total RNA with Ribo-Zero Gold Human/Mouse/Rat (Illumina) was used for removal of rRNA and construction of cDNA library. An Illumina platform was used to generate 101 bp pair-end reads.

Trinity 2.6.6 (Grabherr et al. 2011) was utilized in the de novo assembly and run with R (R Development Core Team 2011) on Taito supercluster (csc.taito.fi). Trimmomatic (Bolger et al. 2014) was run as a Trinity plugin and used in removing adapters and trimming reads. A custom virus protein database was used in the BlastX (NCBI BLAST 2.7.1) homology searches run as parallel BLAST in Taito supercluster. Geneious 10.2.6 (Biomatters Ltd) was used for finding open reading frames (ORFs), aligning contigs as well as mapping the reads against the putative virus contigs (Geneious assembler with medium-low sensitivity). To complement virus discovery using BlastX, we performed an analysis of ORFan-encoding RNA segments (i.e. segments with no detectable homology with fungal or viral proteins, at least 1kb in length, encoding for at least a protein >15kDa, with at least 1000reads/kb mapping the contig, and with abundant accumulation of both positive and negative sense reads).

Motifs and domains were searched with MOTIF search (https://www.genome.jp/tools/motif/). Predicted molecular weight and pI were calculated with ExPASy (https://web.expasy.org/compute_pi/).

Viral contigs of interest were mapped on stranded cleaned libraries to give a more complete overview of the transcriptome complexity. Bowtie2 (Langmead & Salzberg 2012) was used to map reads on viral contigs.

TruSeq Stranded Total RNA technology enables not only whole-transcriptome analysis, but also the precise measurement of strand orientation. SAMtools (Li et al. 2009) extracts the reads mapped on sense or anti-sense viral strands, reporting three numbers for each viral contig: the total reads, the positive sense reads (samtools view -F 0x10) and the negative sense reads (samtools view -f 0x10).

In some analyses, a head-to-tail dimer of the protein was used to map reads and reads mapping across the junction were visualized with Tablet (Milne et al. 2016).

2.4 Validation of *in silico* assembly of virus-like sequences and assignment of specific host isolates

One µg of total RNA was used in the generation of cDNA with random hexamer primers and RevertAid M-MuLV reverse transcriptase (Thermo Scientific). Reverse transcription was conducted according to manufacturer's instructions but with initial denaturation of 2 min at 98 °C for RNA and random hexamer primer and subsequently performing transcription using 10 U RiboLock RNase Inhibitor (Thermo Scientific) and 100 U RevertAid M-MuLV RT. Screening of fungal hosts was performed in standard reverse transcriptase PCR (RT-PCR) with putative viral contig specific primer pairs (Supplementary Table S2) and DreamTaq DNA Polymerase (Thermo Scientific). Next, DNA of virus positive strains was extracted (Turina et al. 2003) and used as a template in standard PCR with contig specific primer pairs (Supplementary Table S2) and OneTaq DNA Polymerase (New England BioLabs) in order to determine whether viral amplicon would originate from fungal DNA. For the virus contigs described in this work a qRT-PCR protocol was implemented exactly as previously described (Chiapello et al. 2020) with oligonucleotides displayed in Supplementary online Table S2.

The two most original and previously unreported genome organizations were confirmed through overlapping RT-PCR and quasi full-length RT-PCR using cDNA as a template that was obtained with a mix of random primers and specific primers used with SuperScript IV RT (Thermo Fisher Scientific) at 55 °C following instructions provided by the manufacturer. PCR amplification was performed with Phusion polymerase (NEB), following manufacturer's suggestions, using extension times ranging from 1 to 4 minutes, according to the predicted length of the amplification product. Oligonucleotides used for this purpose are displayed in Supplementary Table S2.

2.5 Northern blot analysis

Northern blot analysis was carried out on fungal samples extracted as described above and separated on Glyoxal-Hepes agarose gel system as previously described in detail (Ferriol et al. 2018). Ribo-probes were derived with T7 RNA polymerase transcription from cDNA corresponding to specific regions of the viral genomes using radioactive UTP labeled with P^{32} in the reaction mix. We derived cDNA probes cloning PCR products of circa 200-400 bp in pGEM-T easy vector (PROMEGA). In order to obtain minus sense and plus strand probes, both orientations were screened and confirmed by sequencing. Specific primers and position of the probes are displayed in Supplementary online Table S3 and in each figure legend related to virus organization. Hybridization, washes and exposure to film were carried out using ULTRAhyb® Hybridization Buffer (Ambion) as previously described (Ferriol et al. 2018). When loading RNAs for Northern analysis, a total RNA extract of tomato brown rugose fruit virus (ToBRFV)-infected tomato plants was included as a RNA size marker (genomic RNA of 6.3 kb and sgRNA2 of 0.7 kb). Negative controls were isolates of the same or closely related fungal species (included in the RNAseq libraries), which were tested negative based on the RT-PCRs for the specific virus analyzed by Northern blot.

2.6 Phylogenetic analysis

Phylogenetic analysis was carried out by first selecting homologous viral proteins from the databases and identifying a possible outgroup (Supplementary online Table S4). For each distinct set of conserved sequences, alignment was performed with Clustal Omega (Sievers et al. 2011) at the EMBL-EBI services website. Phylogenetic tree were derived with the Maximum likelihood methodology implemented in IQ-tree (Trifinopoulos et al. 2016), choosing the best substitution model (Kalyaanamoorthy et al. 2017) and using the ultrafast bootstrap option (Diep Thi et al. 2018). The substitution model and parameters specific for each tree are detailed in each figure legend.

2.7 5' and 3' RACE

In order to determine the 5' and 3' prime terminal sequence of the two narnavirus-like viral segments and the bunyavirales-like viral segment we performed a RACE protocol as previously described in detail (Rastgou et al. 2009). Briefly, cDNA with specific primers (specifically described in Supplementary online Table S2) was synthesized from total RNA extracted as described above, using SuperScript IV Reverse Transcriptase (Therm-Fisher Scientific). RNase H digestion was performed on cDNA and the ssDNA was purified with a DNA purification kit following specific instructions for ssDNA (DNA Clean & Concentration Kit (Zymo Research)). dGTP and dATP were used to add a polyG or polyA tail using rTdT, terminal deoxynucleotidyl transferase (Promega). The final PCR step was carried out with the Oligo-dC(Eco-bam-dc12) or oligo-dT-V previously described (Rastgou et al. 2009) with specific internal primers (Supplementary online Table S2). We used the same protocol to determine 5' and 3' ends, only changing the virus-specific primers, since the virus we tested accumulated a good amount of both +strand and -strand genomic RNA. PCR product were sequenced directly with specific primers or cloned and sequenced if unspecific amplification products were observed.

2.8 RNase R digestion

RNase R digestion was performed on total RNA extracted from lyophilized mycelia as described above. We used as negative control RNA extracted from tomato infected with ToBRFV. Digestion was carried out on 6 mg of total RNA in a reaction of 20 µl with buffer and conditions suggested by the manufacturer (Epicentre). Each digestion contained 10 U of enzymes. Reactions were carried out for 2 hrs in total, interrupted every 30 min to separate 5 µl and after inactivation (65 °C for 20 min) run in glyoxal HEPES gels as described above.

2.9 Cell fractionation/virus enrichment protocol.

Twenty grams of fresh mycelia (isolate O4) was harvested from a 3-day liquid culture (500 ml) through filtration with Miracloth (Calbiochem). A row extract (EXT) was obtained adding 200 ml of 0.1 Tris pH 8 buffer with EDTA, Na-sulfite and DIECA and homogenizing it in a beat beater for five 60 second rounds (resting for 2 min between each round). A low speed centrifugation (3,000 RPM in a Sorvall GSA rotor) resulted in a supernatant (S1) and a large pellet that was subsequently resuspended in 10 ml of the same buffer (P1). A second low speed centrifugation (10,000 RPM in a Sorvall GSA rotor, using adaptors for Falcon 50 ml conical tubes) resulted in a supernatant (S2) and a pellet, again resuspended in 2.5 ml of 0.1 Tris pH 8. Finally, the supernatant was centrifuged at 36,000 RPM with a Ti55 Beckman rotor for 150 minutes. This resulted in a supernatant (S3) and a final pellet containing the microsomal fraction (P3). Finally, the pellet was resuspended in 2 ml 0.01 Tris buffer pH 7.0. RNA was extracted from equivalents of the original extracts and qRT-PCR on cDNA originating from each fraction was carried out as described above. The P3 fraction was negatively stained and observed at the electron microscope as previously described (Nerva et al. 2016).

3. Results

Our ERM fungal collection included 31 *Oidiodendron maius* strains, isolated either from *Vaccinium* species or from *C. vulgaris* (Supplementary online Table S1) (Read 1974; Couture et al. 1983; Dalpe 1986; Perotto et al. 1996; Lacourt et al. 2000; Martino et al. 2000; Martino et al. 2003; Vallino et al. 2011). The ERM fungi in this study also included two *Rhizoscyphus ericae* strains isolated from *C. vulgaris* roots. This was the first fungal species isolated from ERM roots

(Pearson & Read 1973). The other four ericoid mycorrhizal strains were sterile mycelia isolated from C. vulgaris, two of them taxonomically related to the so-called '*Rhizoschyphus ericae* aggregate' and two belonging to the Helotiales.

Our ORM fungal collection included 12 strains in the genera *Tulasnella* and *Ceratobasidium*, all isolated from the roots of Mediterranean terrestrial orchid species in Italy (Girlanda et al. 2011).

A number of ITS rDNA sequences were determined on selected isolates to confirm previous assignments (not shown). After growing the fungal isolates in axenic conditions, HTS on rRNA-depleted total RNA was carried out on five distinct libraries containing eight to eleven pooled samples each (Supplementary online Table S5). Overall, we obtained ca. 103–118 million pair-end reads for each library and the reads are available in the SRA archive through the BioProject accession number PRJNA629308. A bioinformatic pipeline previously described in detail (Chiapello et al. 2020) allowed us to characterize putative viral contigs present in each library *in silico* and trace each contig to the specific sample by RT-PCR (Supplementary online Table S5). Below are the main findings described according to the fungal host.

3.1 Mycoviruses in ericoid mycorrhizal fungi

After assembling the reads corresponding to each of the libraries of ERM fungi, a first search of a custom-made viral database revealed three putative viral contigs (Table 1). For each putative viral contig, we first investigated their presence in the library by mapping sequencing reads to the viral contigs. Their number is an indication of relative expression and these viruses were all highly abundant in the libraries with high coverage along their genomes (Table 1). We then assigned each putative viral contig to each host isolate by RT-PCR (see Supplementary online Table S5). In some of the *O. maius* isolates we detected two distinct narnavirus-like sequences and one ourmia-like virus (Fig. 1A).

The ourmia-like sequence (contig DN47822) shares the highest BlastX identity (60.7%; query cover 77%) with Combu positive-strand RNA mycovirus (GenBank accession H990636; unpublished), with an E-value of 0. It encodes a single ORF, predicted to be translated into a protein that has a typical RNA-dependent RNA polymerase (RdRP) domain (PFAM code PF05919) with a predicted molecular weight of 72.1 kDa. Phylogenetic analysis shows that it clusters among members of the classified genus *Scleroulivirus* in the family *Botourmiaviridae* (Fig. 1B). For this virus we suggest the name Oidiodendron maius ourmia-like virus 1 (OmOlV1).

The two narna-like viral contigs, DN37559 and DN43802, both have a typical narnavirus-like genome organization, with the potential to express a single protein of circa 88.2 kDa and 89.6 kDa, respectively. However, closer examination of sequence characteristics and host ranges provides strong evidence that the two contigs represent the two genome segments of a bisegmented narnavirus, designated here as 'Oidiodendron maius splipalmivirus 1 (OmSPV1)' for reasons described below. In our culture collection, both contigs are present in three *O. maius* isolates originating from different mycorrhizal plants growing in the same non-polluted site and representing different clonal individuals (Supplementary online Table S5). For the first putative narna-like contig (DN37559), the closest hit in the NCBI database is that of the RdRP of Plasmopara viticola lesion associated narnavirus 20 (unpublished, GenBank QIR30299.1) with 48.6% identity and a coverage of 86%. For the second narna-like contig (DN43802) there is a unique hit in the viral database, Beihai narna-like virus 22 (Shi et al. 2016), with 26% identity on a very limited part of the genome (23% coverage) and an E-value of 0.09 (Table 1). Phylogenetic analysis includes DN37559 in a distinct clade with other narna-like unassigned viral sequences

(Osaki et al. 2016; Zoll et al. 2018; Nerva et al. 2019a) very distantly related to *Leviviridae* and *Narnaviridae* using both a Maximum Likelihood (Fig. 1B) and a Bayesian methodology (Supplementary online Fig. S1); DN43802 was not included in the dendrogram because the sequence was too divergent from known taxa to allow reliable phylogenetic inference. Domain analysis with MOTIF Search (https://www.genome.jp/tools/motif/) for both DN37559 and DN43802 failed to detect the signature of a typical RdRP. Alignment of DN37559 ORF1-encoded protein with a number of other virus RdRPs (for which the evolutionary divergence value is below an acceptable threshold) confirms the presence of homologues of the motif A and B of the palm domain but the absence of the GDD-carrying C domain at their carboxy terminal (Supplementary online Fig. S2)(te Velthuis 2014).

Given the lack of a complete and recognizable RdRP palm domain, we further characterized these two putative virus segments to exclude that one or more copies of cDNA corresponding to these RNA segments were endogenized in the *O. maius* genome and, at the same time, to confirm that these are RNA viruses and do not have a DNA replication intermediate or a DNA genome. Blast search of the DN37559 and DN43802 sequences in the strain whose genome was previously sequenced (Kohler et al. 2015) failed to retrieve any hit, therefore excluding the possibility of endogenization. In addition, quantitative PCR experiments on total nucleic acid did not amplify a small fragment of the putative viral genome. Thus, we could exclude a DNA intermediate during replication (Fig. 1C). We then performed a RACE protocol to determine the exact ends for both DN37559 and DN43802 genomic RNAs; both contigs shared a poly(U) leader at the 5' end, of different variable length (8-12 nt) according to the different cDNA clones sequenced, with two variable nucleotides as terminal nucleotides. At the 3' end, both viral contigs shared a poly(A) tail of variable length (8-10 nt) with two variable nucleotides as sequence termini.

Noticeably, the region of identical nucleotides in the alignment extends downstream of the 5' poly(U) stretch (28 nt) and upstream of the poly(A) stretch (Fig. 1D) strongly suggesting that the two genomic segments are from the same virus (replicated by the same viral RdRP).

To further characterize the nature of these two segments, we checked the number of positive sense and minus strand reads mapping against the genome (Table 2). Surprisingly, a higher number of reads mapped to the negative strand, suggesting that for these virus-like segments, a higher abundance of negative strand RNA accumulates. As a control, we mapped *O. maius* actin, tubulin and ATPase reads on the putative transcript and found the expected accumulation of—almost exclusively—plus strand reads. Furthermore, we also included in the analysis OmOlV1 and it accumulates more plus strand reads than minus strand, as expected from plus strand genome viruses (Table 2). Northern blot analysis confirmed the abundant accumulation of DN37559 and DN43802, with genomes of the expected size, and a stronger signal of the minus strand genomic RNA compared to the plus strand RNA for both DN37559 and DN43802, more evident for DN43802 (Fig. 2 and Supplementary online Fig. S3).

Finally, given the uniqueness of the DN43802 contig, we searched homologues of this virus segments in some Trinity assembly databases for filamentous fungi from our previous works (Nerva et al. 2016; Nerva et al. 2019a; Nerva et al. 2019b) and from a number of fungal transcriptomes available in public databases. We were able to retrieve four putative DN43802 homologous protein sequences: two from esca disease-associated fungi, one from *Holothuria polii*-associated fungi and one from the basidiomycete *Wallemia sebi* (isolate MUT4935) associated with *Posidonia oceanica* (Nerva et al. 2016; Nerva et al. 2019a; Nerva et al. 2019b). Protein sequence alignment shows that these viral sequences, as well as DN43802, align with

the N-terminal region of a much larger putative RdRP of the distantly related Beihai narna-like virus 22 (Shi et al. 2016). This region contains the specific C and D subdomain of the putative RdRP (Fig. 3). Given the possible strict association of the two virus segments in our *O. maius* collection (they are in the same libraries and in the same samples, and with identical 5' and 3' ends), we re-examined the libraries that harbor the homologues of DN43802 (i.e. esca disease-associated fungi, *Holothuria polii*-associated fungi, and *Wallemia sebi* isolate MUT4935) for homologues of DN37559. Indeed, we were able to retrieve the corresponding DN37559-like protein encoding segments (Fig. 3). Finally, we were able to trace, through a specific qRT-PCR assay, the presence of the two virus segments found in the *H. polii*-associated fungi to a specific fungal isolate, *Penicillium stoloniferum* MUT2120.

Overall, in five distinct libraries/samples (Fig. 3) we were therefore able to strictly associate, in a putative single virus genome, two virus segments—one that carries the A and B subdomain of the RdRP palm domain at the carboxy terminal of the protein (DN37559-like) and one that carries the C and D subdomain containing the GDD triplet and a conserved K residue, respectively, at the amino terminal of the protein (DN43802-like). Some other lateral conserved domains were also detected following the nomenclature previously used (subdomain I to VIII, Fig. 3) (Koonin 1991). In conclusion, the results indicate that the DN37559 and DN43802 contigs represented the two genome segments of a single virus named after its unique split palm domain as 'Oidiodendron maius splipalmivirus 1'.

3.2 Mycoviruses in orchid mycorrhizal fungi

In the collection of ORM fungal isolates, all belonging to the genera *Ceratobasidium* and *Tulasnella* (Basidiomycota), we found a variety of viruses, some of which are new viruses belonging to putative new species in classified virus families; a detailed description of these viruses is provided in Supplementary on line Appendix-I and related Supplementary online Fig. S4. Briefly, these viruses could be affiliated with virus families *Barnaviridae*, *Endornaviridae* and *Mitoviridae* (Table 1).

Besides these well-known virus taxa, one virus contig (DN37204), only found in a single *Tulasnella* isolate (O7), had a surprising unprecedented genome organization. A 12 kb RNA fragment comprises three ORFs (Fig. 4A): the largest one encodes a putative RdRP of 290,3 kDa calculated molecular mass, and the closest match by BLASTp was with the RdRP of Hubei orthoptera virus 2 (E value 1e-07, identity 23%, query coverage 8%) and Guaroa virus (Orthobunyavirus). Both these viruses are multisegmented, and the RdRP is the only protein encoded by the largest of their genomic segments. This protein carries the typical motif of a bunyavirus RdRP (pfam04196, Bunya RdRP). The second largest protein is encoded by the same genome strand (arbitrarily antisense, since RdRP is antisense in *Bunyavirales*) and has a predicted molecular mass of 129,3 kDa. Although we found no specific hits for this protein in the viral database, it carries the Tom22 motif (a protein of the mitochondrial translocase family), with a relatively high E-value of 0.013. Finally, the third ORF encodes, in the sense orientation, a putative nucleocapsid protein (PF02477, Nucleocapsid Nc protein) of 27.8 kDa, that shares some similarity with the Nc of Largemouth bass bunyavirus (Supplementary online Fig. S5A). For this putative virus, we propose the name Tulasnella bunyavirales-like virus 1 (TuBlV1). Phylogenetic analysis indeed placed this new virus fragment inside the *Bunyavirales*, but its assignment to existing clades is not supported statistically (Fig. 4B).

Given the surprising genome organization for a member of the *Bunyavirales* (three ORFs encoded by a single segment), we searched for evidence that the 12 kb contiguous RNA

segment exists as a molecule and was not simply assembled *in silico* due to the 5'–3' complementary sequences present in general in multisegmented members of the *Bunyavirales* (that are sometimes assembled in a single sequence). We therefore amplified overlapping segments through RT-PCR spanning the whole genome length (Fig. 5A) and we could indeed confirm the presence of such predicted contiguous RNA. Furthermore, display of the reads mapping on the full-length genome revealed a rather uniform distribution, with several reads validating the link between ORF1 and ORF2 position, and the intergenic region between ORF2 and ORF3 (Supplementary online Fig. S5B). Northern blot analysis showed indeed the presence of a large genomic segment with each of the three probes, thus confirming the existence of the circa 12 kb RNA genomic segment (Fig. 5B). In one RNA sample, a small RNA specifically hybridizing with the putative minus strand probe was also visible, and its size is consistent with a possible subgenomic RNA (Supplementary online Fig. S6A) corresponding to the nucleocapsid coding RNA. Table 2 shows the number of reads mapping to the genomic (+sense reads) and antigenomic (negative sense reads) for the overall genomic segment and for the three coding regions, separately. Overall, we found more negative sense reads, and only the Nc coding region had an excess of plus strand reads, which suggests a specific subgenomic RNA as expression strategy for this portion of the genome. Furthermore, a U-rich region of circa 40 nt was found after the putative Nc stop codon, a possible signal for transcription termination.

We also checked, through PCR amplifications on total nucleic acid extracts, for the possibility that this virus could be integrated in the fungal genome, but failed to detect any specific product, thus confirming that this is a putative replicating viral segment depending on viral RdRP activity (Supplementary online Fig. S6B).

Finally, to complement virus discovery using BlastX, we performed an analysis of ORFan-encoding RNA segments (i.e. segments with no detectable homology with fungal or viral proteins). In the XEO library we initially detected two contigs (DN30310 and DN33730) of circa 4.7 kb, each encoding two ORFs arranged in an ambisense (but pointing outward) coding strategy. These two ORFs (hereafter ORFA and ORFB) were predicted to encode proteins that had no conserved homology with any protein in the viral database, except for two orphan proteins in the nr database from *Agaricus bisporus* (Table 1). Such proteins were encoded by an ORFan segment detected in a previous study, but not included by NCBI in the viral database (Deakin et al. 2017). By specific qRT-PCR, we assigned each of the two putative 4.7 kb virus segments to ORM fungi in the genus *Tulasnella* (Supplementary Table S5 and Supplementary online Fig. S7A). The specific contig DN30310 was abundant (ct 14 in qRT-PCR) in *Tulasnella* isolate O10, whereas contig DN33370 was less abundant in three *Tulasnella* isolates, O7, O11, and O12 (Supplementary online Table S5). A graphic representation of the main genomic features of these putative viral contigs is displayed in Fig. 6A. We named these two putative viruses Tulasnella ambivirus 1 and Tulasnella ambivirus 2 (TuAmV1 and TuAmV2, respectively). Given the surprising and unprecedented genomic organization of the segments assembled *in silico*, we checked by RT-PCR (overlapping fragments and nearly full length) if the RNA segment existed as a full-length sequence. RT-PCR revealed that indeed such segments existed as predicted *in silico* (Supplementary online Fig. S7B and C).

We then proceeded to investigate the presence of RNA transcripts (contigs) homologous to the TuAmV1 and TuAmV2 found in the XEO library in the other ERM and ORM fungal libraries described in this work. Homologous segments were absent in ERM fungi but were found in the other ORM fungal libraries. In detail, four putative full-length segments were identified and associated with specific isolates of *Tulasnella* and *Ceratobasidium* (Supplementary online Table S5), whereas two more segments were likely only partial genomes. We named these new viruses

Ceratobasidium ambivirus 1 (CeAmV1=contig DN43545), Tulasnella ambivirus 3, 4, 5 (TuAmV3, TuAmV4, TuAmV5, respectively contigs DN37145, DN32762, and DN36670); the two partial genomes belong to Tulasnella ambivirus 6 and 7 (contigs DN36393 and DN36572). In all cases, the genomic organization of the contig assembled *in silico* is ambisense, but in one case the two ORFs point inward, as is common for other ambisense segments in negative stranded RNA viruses (Supplementary online Fig. S8). The Trinity-assembled contig DN43545 had a length of 9.8 kb, but a closer inspection revealed that the contig was an almost complete dimer (Supplementary online Fig. S10C) and that the monomeric sequences were similar, in length and genome organization, to the others retrieved.

The unusual ambisense genomic organization is also supported by the number of overlapping reads mapping across the full-length genome visualized with Tablet (Supplementary online Fig. S9). DNA corresponding to the RNA segment could not be detected by a sensitive qPCR assay in any of the isolates carrying these two virus genomic segments (Supplementary online Fig. S10A) therefore excluding i) that they are transcripts derived from a DNA genome, ii) that they are transcripts derived from endogenization of an RNA virus or iii) that their replication occurs through a DNA intermediate.

Given the number of different ambiviruses found in our collection of ORM fungi, all having a genome with RNA molecules between 4 and 5 kb in length, we could align the respective deduced encoded proteins (ORFA-like and ORFB-like) and revealed that they were both fairly conserved. ORFA encodes a protein with a well conserved domain centered around a GDD motif, as is the case with most of the RdRPs of RNA viruses (te Velthuis 2014) (Fig. 6B). Also, some other well conserved key residues of other RdRP domains were present, but insufficient to be detected as RdRP domains with the current motif search engines (MOTIF Search at https://www.genome.jp/tools/motif/). Overall, the estimate of the evolutionary divergence among aligned ORFA proteins was 0.66 (for specific pairs see Supplementary online Fig. S11A). ORFB-encoded proteins were also conserved among different isolates, but less than ORFA-encoded proteins (estimate of the average of evolutionary divergence is 0.72). Some residues were conserved among all isolates so far described, but this protein remains with no assigned function at this time (Supplementary online Fig. S11B). Given the limited conservation with other viral RdRP, a phylogenetic tree that includes them would not be reliable (Holmes & Duchene 2019).

The prevalence of this new putative viral genomic segment in many of our *Tulasnella* isolates prompted us to search for homologues in libraries we previously published from other filamentous fungi: one homologous viral fragment was retrieved from library F4 from the esca disease-associated fungal collection (Nerva et al. 2019a). The main features associated to this virus fragment are in Supplementary online Fig. S12.

The existence of closely related ambisense contigs having opposite orientation, inward and outward (Fig. 6 and Supplementary online Fig. S8), suggested the possibility that they are alternative assembly forms originating from a circular RNA molecule, or from a head-to-tail dimer molecule originated as a replication intermediate. We looked for evidence of such molecules by RT-PCR across a putative circularized junction (and by visualization of reads mapping across the putative junction). Both approaches (Supplementary online Fig. S9 and S10B and S10C) supported the possibility of a circular or dimer replication intermediate (in comparison with mapping of a traditional plus strand RNA segment).

Northern blot analysis with positive and negative sense probes corresponding to each of the two ORFs was carried out for two viruses, TuAmV1 and CeAmV1 (found in O10 and O4 isolates,

respectively). Surprisingly, the two viruses yielded a different banding pattern. In the case of TuAmV1, the four probes reacted specifically with a single RNA of the expected genomic size (Fig. 7A). In the case of CeAmV1, the most abundant band has an estimated size consistent with a putative dimer of the genomic segment, which is instead present at lower concentration (Fig. 7B). We could not reveal the existence of subgenomic RNAs. A difference between TuAmV1 and CeAmV1 was also observed in relation to positive sense and minus sense mapping reads: we arbitrarily assigned plus strand orientation to the RNA that encodes for ORFA, the putative RdRP, and minus strand to the opposite orientation; in the case of TuAmV1, we detected more plus strand reads, whereas the contrary was true for CeAmV1 and all the other ambiviruses (Supplementary online Table S6).

We then proceeded with an RNase R assay to check if these RNAs were sensitive to its exonuclease activity. A time course shows that the RNA was completely degraded 30 min after adding the enzyme, like a ToBRFV control we included in the experiment, thus suggesting that these RNA species might not be circular (Supplementary online Fig. S13).

Finally, a cell fractionation protocol was performed in order to check in which fraction the virus RNA was most enriched: viral RNA did not sediment after low speed centrifugations, but accumulated mostly in the microsomal fraction (in the pellet of a high speed centrifugation, after rounds of differential centrifugations) (Supplementary online Table S7). Despite its accumulation in the microsomal fraction, we were not able to see any specific virus-like morphology associated with the presence of the RNA in this fraction.

4. Discussion

The close and evolutionarily long-term association between mycorrhizal fungi and their host plants offers a wide temporal window for possible inter-kingdom horizontal virus transfers and selection of mycoviruses with a potential beneficial role in the tripartite interactions involving mycoviruses, mycorrhizal fungi and host plants. However, a prerequisite for testing these hypotheses is the comprehensive description of the viromes associated with mycorrhizal fungal isolates. In the present study, we describe the virome of a collection of ERM and ORM fungi that results in the discovery of surprising new evolutionary lineages that extend the boundaries of homology-based searches of RdRP conserved domains. Our work reports, for the first time, mycoviruses associated with ERM fungi and increases the diversity of mycoviruses characterized in ORM fungi (Ong et al. 2016; Ong et al. 2017; Ong et al. 2018). In addition to new viruses related to established taxa, we present three virus types with unprecedented genome organizations, one of which represents a completely new virus group that was not possible to reliably include in the monophyletic phylogenetic tree comprising the vast majority of RNA viruses (Wolf et al. 2018). The ICTV currently includes all viruses with an RNA genome in the realm *Riboviria*, and those that specifically use an RdRP for their replication are in the kingdom *Orthornavirae*. The five branches in the *Orthornavirae* monophyletic tree are now recognized as phyla: the *Lenarviricota* (levi-narna-ourmia-mito-like viruses), the *Pisuviricota* (the picornavirus supergroup), the *Kitrinoviricota* (including the alphavirus and flavivirus supergroup), the *Duplornaviricota* (including a number of dsRNA virus clades) and the *Negarnaviricota* (including viruses with (-)RNA virus genomes) (Koonin et al. 2020). The viruses from our current study that could be reliably placed in this monophyletic tree belong to the *Lenarviricota*, *Kitrinoviricota* and *Negarnaviricota*.

4.1 Discovery of a novel split organization of the palm domain in two genomic viral segments

The ERM fungi harbored two distinct narna-like contigs, DN37559 and DN43802, which showed some conservation with Plasmopara viticola lesion associated narnavirus 20 (unpublished, GenBank QIR30299.1) and Beihai narna-like virus 22 (Shi et al. 2016), respectively. However, a closer inspection of DN37559, DN43802 and Beihai narna-like virus 22 alignments revealed that the two lenar-like contigs hosted by ERM fungi aligned to different regions of the RdRP of Beihai narna-like virus 22. Unexpectedly, DN37559 harbored the A and B subdomain of the palm domain at the carboxy-terminus, whereas DN43802 contained the C and D subdomains at its amino terminus. A number of viruses with the same domain organization as that of DN37559 have already been detected *in silico* in previous works (Osaki et al. 2016; Zoll et al. 2018; Nerva et al. 2019a), but only in a recent report was the absence of the important GDD carrying C subdomain noticed (Lin et al. 2020). For most of these lenar-like viruses, neither the raw reads nor the transcriptome assembly were deposited in public databases, and it was therefore impossible to verify a hypothesis of strict association of DN37559- and DN43802-type segments, with the exception of a library of fungi associated with esca disease with reads deposited in SRA archives (Nerva et al. 2019a), where a homologue of DN43802 was indeed found. Furthermore, we found in transcriptomic libraries from our previous works the same combination of DN37559-type and DN43802-type homologous segments showing that these viruses are not specific to *O. maius*, but can be found in both asco- and basidiomycetes.

A comprehensive phylogeny of RNA viruses is based on the viral RdRP universally conserved module, which includes at least the A, B and C subdomains. Here we show for the first time that such subdomains can be encoded by two distinct genomic segments: subdomain A and B from an DN37559-type of virus segment and C from an DN43802-type of segment. Previously, an exception to the A-B-C subdomain module was reported, showing a circular permutation of the order of the domains (C-A-B) in *Permutotetraviridae* and *Birnaviridae* families (Gorbalenya et al. 2002). Nevertheless, also in this case, the palm domain was encoded by a single protein. We can safely exclude that splitting of the coding sequence in two contigs is due to an assembly or sequencing artefact because i) we could confirm the size of each segment by Northern blot, ii) we could complete a RACE experiment with both viruses, iii) the read coverage is very high, and iv) the same single contigs are reported independently from different works. The highly conserved sequences in the 5' and 3' UTR support the notion that the two sequences constitute the genome of a single, bisegmented virus for which we suggest the name Oidiodendron maius splipalmivirus 1 (OmSPV1). Splipalmiviricetes/splipalmiviridae is the tentative name of a taxon (likely a new class or new family) that accommodates this new clade of viruses (name derived from SPLIt PALM domain viruses). Bi-partitism in some narnaviruses was first inferred from metagenomic studies (Shi et al. 2016) and was recently confirmed to be a feature of some protozoa and apicomplexan-infecting viruses (Charon et al. 2019). Nevertheless, in such cases the RdRP palm domain is present in a single protein encoded by one of the two viral genomic segments, while the other segment codes for proteins of unknown function.

This observation can be extended to the thousands of RNA viruses so far characterized. To our knowledge, there is no precedent for a splitting of the RdRP into two distinct proteins. This raises a question about the possible evolutionary trajectory of these viruses. Judging from their very distant relationship from existing RNA viruses, it might be tempting to hypothesize that they are basal to narnaviruses. Alternatively, it is also possible that having the palm subdomains encoded by different proteins might alleviate some of the structural constraints that are present in the

single protein-encoded ABC palm subdomain, allowing faster evolution after separation of the domains.

Another interesting feature of these viruses is the fact that, for both segments, there is a higher accumulation of the (-)RNA (arbitrarily assigning the plus strand to the one encoding the RdRP, as for other narnaviruses). This is a new feature (confirmed by strand-specific Northern blot analysis) that has never been reported before in any other putative (+)RNA. Viruses are defined as carrying a plus or minus strand genome based on the fact that encapsidated RNA respectively can or cannot function as messenger RNA once they are released in the cell: given that narnaviruses are capsidless naked RNA virus-like agents, such definition does not apply.

Narnaviruses were first discovered in baker's yeast, where it was not possible to associate any phenotypic change with their presence-absence (Kadowaki & Halvorson 1971; Wesolowski & Wickner 1984; Hillman & Cai 2013). The recent evidence that narnaviruses can infect not only fungi but also insects (specifically dipteran) (Chandler et al. 2015; Goertz et al. 2019), other arthropods (Shi et al. 2016), a brown alga (Waldron et al. 2018), trypanosomatids (Grybchuk et al. 2018) and nematodes (Richaud et al. 2019) has raised further interest in these viruses. Moreover, a recent work has shown their effect on the reproductive fitness of their Mucoromycota host *Rhizopus microsporus* in a tripartite interaction with an endobacterium that is involved in virulence toward the plant host (Espino-Vazquez et al. 2020). The ERM strains hosting OmSPV1 have been isolated from *C. vulgaris* from a heathland area in Northern Italy and are genetically close but distinct (Perotto et al. 1996). Indeed, the success of ericaceous shrubs in heathland habitats, which can be very poor in nutrients and high in toxic metal ions, is due to their endomycorrhizal association (Bradley et al. 1982). The finding of viral sequences in such strains poses the question of whether they might play a role in the fungus-plant, fungus-environment and plant-environment interaction, in analogy with the thermal tolerance observed for a tripartite interaction plant-fungal endophyte-virus (Márquez et al. 2007).

In ERM fungi, we also found a new species of ourmia-like virus, with characteristics similar to ourmia-like mycoviruses already characterized in other fungi. This group of viruses has gained some attention because it shows evidence of evolutionary exchanges between different kingdoms (Rastgou et al. 2009). Fungal isolates E35 and E36 (hosting OmOIV1) originate from distinct soil plots within the same polluted area (Lacourt et al. 2000; Martino et al. 2003, Vallino et al. 2011) and have been found to tolerate heavy metals (Zn and Cd, respectively) (Vallino et al. 2011). An ourmia-like virus was shown to be associated with mitochondria (Hrabáková et al. 2017) and this fact can provide a possible functional link between virus presence and heavy metal tolerance, since mitochondria are central to heavy metal tolerance in fungi (Daghino et al. 2019). The possibility to transfect *O. maius* protoplasts with transcripts from a putative infectious clone will help determine if OmOIV1 indeed bears a role in heavy metal tolerance.

4.2 An unprecedented tri-cistronic RNA related to members of *Bunyavirales* encodes both a putative RdRP and a putative Nc on the same viral segment

The virome of ORM fungi has been a subject of a pioneering study that revealed the presence of dsRNA that did not result in a specific taxonomic assignment (James et al. 1998). Investigations carried out on natural populations of orchids from Australia revealed i) several new endornavirus species and a new endornavirus genomic organization (Turina et al. 2018), ii) ten partitiviruses from *Ceratobasidium* spp. (Ong et al. 2017), and iii) a mitovirus, a hypovirus, two dsRNA viruses, a toti-like virus and a megabirna-like virus also from *Ceratobasidium* spp. (Ong et al. 2018).

To this already vast array of viral sequences, we add here a new mitovirus, a new barnavirus and two new endornaviruses, all related to those already found but different enough to be considered new species. In addition, for the first-time a minus stranded RNA virus, TuBlV1, was detected in ORM fungi. Phylogenetic analysis of the RdRP encoded by this virus shows that it belongs to the *Bunyavirales* order, but its genome has some unique features that expand the diversity of genome organizations so far characterized in this order. We demonstrate the existence of a single genomic segment that also encodes, together with the RdRP, another small ORF in the ambisense orientation (genomic sense) and a third ORF that terminates just upstream of the RdRP, in the same antisense orientation and with no intergenic region.

In the *Arenaviridae*, only the *Mammarenavirus* and *Reptarenavirus* genera have an RdRP encoding segment that also encodes for a second ORF in the ambisense orientation, a small matrix protein (Perez et al. 2003), and this is so far a unique feature inside the hundreds of viruses characterized in the *Bunyavirales* (Shi et al. 2016; Kaefer et al. 2019). Nevertheless, we show evidence that in the case of TuBlV1 the protein encoded in the ambisense orientation is not a matrix protein but a nucleocapsid protein, whereas in the case of the bipartite arenaviruses the nucleoprotein is encoded by a different genomic segment, as is the case in all previously known members of the *Bunyavirales*. Also puzzling is the presence of the third ORF upstream of the RdRP. We confirmed this occurrence in a contiguous RNA both by sequencing the RT-PCR product across the junction and by Northern blot analysis. A careful look at the reads mapping across the junction also confirms the uniformity of the sequence in that region without any detected variants. The last nucleotide encoding ORF3 is the first nucleotide of the RdRP, opening the possibility of a -1 frameshift as an expression strategy of the RdRP encoding ORF or of a re-initiation expression strategy.

Phylogenetic analysis also shows that this virus does not belong to any of the existing or proposed clades in the *Bunyavirales*, including also a number of recently characterized phlebo-like mycoviruses (Nerva et al. 2019b; Chiapello et al. 2020); therefore a new taxon should be assigned to accommodate TuBlV1.

4.3 Orchid mycorrhizal fungi harbor ambiviruses, an ORFan group of ambisense bicistronic viruses that cannot yet be assigned to the viral RdRP monophyletic phylogenetic tree.

In our collection of ORM fungi, we serendipitously found a number of distinct virus sequences, characterized by a bicistronic ambisense RNA segment of circa 5 kb with both ORFs conserved among the discovered virus segments; these features define a new virus clade with no detectable relationship with existing characterized viruses. Nevertheless, we could show that they are replicated via a minus strand/plus strand RNA replication cycle that does not entail a DNA phase. The surprising ambisense orientation of the ORFs encoded by these genomes have so far only been shown for the *Bunyavirales* and more recently for some narna-like sequences (DeRisi et al. 2019; Dinan et al. 2020), although in this case the evidence is indirect, and the two ORFs overlap. We could not show evidence of subgenomic RNA accumulation, but relatively abundant accumulation of both plus strand and minus strand orientation of the genomic RNA could suggest that the genomic and antigenomic RNA can express both proteins. Furthermore, both proteins (ORFA- and ORFB-derived) are highly conserved among the different isolates, suggesting a function related to viral replication. Since the assembly of ambivirus contigs by Trinity software was in some cases prone to some artifacts, leading to arbitrary assembling of contigs as dimers with a number of reads across the putative junction, we deposited the putative ambivirus genomes as monomeric sequences. Our results indicate that abundant accumulation of the dimer

is not a prerequisite of the replication cycle because one of these ambiviruses (TuAmV1) does not accumulate the dimer as shown by Northern blot. Abundant genomic dimer accumulation was previously shown for some specific bunyavirus-host combinations (Bertran et al. 2016), and their significance as defective interfering RNA that regulate accumulation of the genomic RNA was hypothesized. A likely misassembly due to the continuum of virus reads mapping across a dimer also occurred when a contig expressing an ORF (with homology to ORFB of ambivirus) was first found in *Agaricus bisporus* (ORFan 1, GenBank ID KY357519) (Deakin et al. 2017). The ORFan 1 includes five ORFs in addition to the one showing homology to ORFB of ambivirus and ORFA is fragmented, possibly due to contig misassembly. The authors found ORFan 1 in two of their isolates at very low transcript accumulation, and thus, ORFan 1 was deposited in GenBank as an *Agaricus bisporus* sequence, therefore not included in any viral database. Here, we provide for the first time evidence that homologues of this ORFan are viral genomic fragments encoding a putative RdRP.

In fact, even though a motif scan search of the two ORFs encoded by the ambivirus did not detect any conserved motif, a closer inspection of conserved motifs in protein alignments of ORFAs suggests the possible existence of an uncanonical RdRP palm domain. As discussed above, motifs A, B and C subdomains are crucial for enzyme activity. To find evidence suggesting the RdRP nature of ORFA from ambiviruses, we aligned ORFAs from all the ambiviruses discovered in the work with a group of different RdRPs hosting the canonical disposition previously used for detecting motifs A, B and C permutation (Gorbalenya et al. 2002). Results show that motif C (hosting the hallmark motif GDD) is aligned correctly with the GDD triad from ambiviruses, while a partial match is found for motifs A and B. Subdomain A usually hosts a conserved D residue with another D residue separated by four or five amino acids (D-X5-4-D); the second of these D residues is not conserved in *Mononegavirales* and *Bunyavirales* (te Velthuis 2014). ORFA proteins encoded by ambiviruses show only the first conserved D residue and the F residue in position +4, which is the most common amino acid in +strand RNA viruses therefore mixing features of both plus strand and minus strand RdRP in this subdomain (te Velthuis 2014). Motif B shows three conserved residues: G, T and N in plus strand RNA viruses, separated by non-conserved amino acids (G-X2-3-T-X3-N). In this case, a partial similarity to ambivirus ORFA could be found with the conserved G residue. However, instead of T and N, the conserved G residue of ORFA was followed by a second conserved G residue in position +3, and N and ST conserved residues downstream.

In conclusion, partial conservation could be observed between the active site of viral RdRPs and conserved motifs of ambivirus ORFA products, with A and C putative subdomains more closely related to +strand (and -strand) RNA viruses, while subdomain B is less recognizable, with a number of conserved residues that match poorly to subdomain B from other viruses. Despite this variability and the chimeric nature of the ABC subdomains in the ambivirus, the three amino acid residues that are invariant (D in subdomain A, G in subdomain B and D in subdomain C) are indeed conserved: in particular, the two aspartic acid residues can interact with two Mg++ ions in the catalytic core of the domain, whereas the glycine in subdomain B is necessary for nucleotide selection (Steitz 1998). Attempts at purifying virus particles or nucleocapsids associated with this virus segment failed, but the viral RNA enriches in the microsomal fraction, as it is the case of other capsidless viral elements (Jacob-Wilk et al. 2006).

Conclusions

The virome in our collection of ERM and ORM fungi featured known mycoviruses as well as novel viruses not previously described in fungi. The identification of new viruses in mycorrhizal fungi expands the boundaries of characterized RNA virus diversity and raises the question of whether

mycorrhizal fungi may represent a special ecological niche for these novel viruses. A more extensive search in fungi with different lifestyles will clarify this point.

Acknowledgments
We thank Riccardo Lenzi, Andrea Delliri, and Caterina Perrone for technical assistance and Prof. Bryce Falk (UC-DAVIS, USA) for critical discussion of the results. Suvi Sutela and Eeva Vainio were supported by the Academy of Finland (grant number 309896). Marco Forgia was supported by a Ph.D. fellowship by MIUR.

References

Andika, I. B. et al. (2017). 'Phytopathogenic fungus hosts a plant virus: A naturally occurring cross-kingdom viral infection', *Proceedings of the National Academy of Sciences of the United States of America,* 114: 12267-72.

Bai, I. X. et al. (1997). 'The ectomycorrhizal basidiomycete *Hebeloma circinans* harbors a linear plasmid encoding aDNA-and RNA polymerase', *The Journal of general and applied microbiology,* 43: 273-9.

Bao, X. and Roossinck, M. J. (2013). 'Multiplexed interactions: viruses of endophytic fungi', *Advances in Virus Research, Vol 86: Mycoviruses,* 86: 37-58.

Bertran, A. et al. (2016). 'Host-specific accumulation and temperature effects on the generation of dimeric viral RNA species derived from the S-RNA of members of the Tospovirus genus', *Journal of General Virology,* 97: 3051-62.

Bian, R. L. et al. (2020). 'Facilitative and synergistic interactions between fungal and plant viruses', *Proceedings of the National Academy of Sciences of the United States of America,* 117: 3779-88.

Blattný, C. and Králík, O. (1968). 'A virus disease of *Laccaria laccata* (Scop. ex Fr.) Cooke and some other fungi', *Ceska Mykologie,* 22: 161-6.

Bolger, A. M., Lohse, M. and Usadel, B. (2014). 'Trimmomatic: a flexible trimmer for Illumina sequence data', *Bioinformatics,* 30: 2114-20.

Bonfante, P. and Genre, A. (2010). 'Mechanisms underlying beneficial plant-fungus interactions in mycorrhizal symbiosis', *Nature Communications,* 1: 48.

Bradley, R., Burt, A. J. and Read, D. J. (1982). 'The biology of mycorrhiza in the Ericaceae. VIII. The role of mycorrhizal infection in heavy metal resistance', *New Phytologist,* 91: 197-209.

Chandler, J. A., Liu, R. M. and Bennett, S. N. (2015). 'RNA shotgun metagenomic sequencing of northern California (USA) mosquitoes uncovers viruses, bacteria, and fungi', *Frontiers in Microbiology,* 6.

Charon, J. et al. (2019). 'Novel RNA viruses associated with *Plasmodium vivax* in human malaria and *Leucocytozoon* parasites in avian disease', *Plos Pathogens,* 15.

Chiapello, M. et al. (2020). 'Putative new plant viruses associated with *Plasmopara viticola*-infected grapevine samples', *Annals of Applied Biology,* 176: 180-91.

Couture, M., Fortin, J. A. and Dalpe, Y. (1983). *'Oidiodendron griseum* Robak: an endophyte of ericoid mycorrhiza in *Vaccinium* spp.', *New Phytologist,* 95: 375-80.

Daghino, S. et al. (2019). 'Yeast expression of mammalian Onzin and fungal FCR1 suggests ancestral functions of PLAC8 proteins in mitochondrial metabolism and DNA repair', *Scientific Reports,* 9: 6629.

Dalpe, Y. (1986). 'Axenic synthesis of ericoid mycorrhiza in *Vaccinium angustifolium* Ait. by *Oidiodendron* species', *New Phytologist,* 103: 391-96.

Deakin, G. et al. (2017). 'Multiple viral infections in *Agaricus bisporus* - Characterisation of 18 unique RNA viruses and 8 ORFans identified by deep sequencing', *Scientific Reports,* 7: 2469.

Dearnaley, J. D., Martos, F. and Selosse, M.A. (2012). '12 orchid mycorrhizas: molecular ecology, physiology, evolution and conservation aspects', *Fungal associations.* Springer: 207-30.

Derisi, J. L. et al. (2019). 'An exploration of ambigrammatic sequences in narnaviruses', *Scientific Reports,* 9: 17982.

Dieleman-Van Zaayen, A., Igesz, O. and Finch, J. T. (1970). 'Intracellular appearance and some morphological features of virus-like particles in an ascomycete fungus', *Virology,* 42: 534-7.

Diep Thi, H. et al. 'UFBoot2: improving the ultrafast bootstrap approximation', *Molecular Biology and Evolution,* 35: 518-22.
Dinan, A. M. et al. (2020). 'A case for a negative-strand coding sequence in a group of positive-sense RNA viruses', *Virus evolution,* 6: veaa007.
Donaire, L. and Ayllon, M. A. (2017). 'Deep sequencing of mycovirus-derived small RNAs from *Botrytis* species', *Molecular Plant Pathology,* 18: 1127-37.
Espino-Vazquez, A. N. et al. (2020). 'Narnaviruses: novel players in fungal-bacterial symbioses', *Isme Journal*, 14: 1743–54.
Ferriol, I. et al. (2018). 'The Torradovirus-specific RNA2-ORF1 protein is necessary for plant systemic infection', *Molecular Plant Pathology,* 19: 1319-31.
Gange, A. C. et al. (2019). 'Meta-analysis of the role of entomopathogenic and unspecialized fungal endophytes as plant bodyguards', *New Phytologist,* 223: 2002-10.
Ghabrial, S. A. (2015). '50-plus years of fungal viruses', *Virology,* 479: 356-68.
Girlanda, M. (2011). 'Photosynthetic mediterranean meadow orchids feature partial mycoheterotrophy and specific mycorrhizal associations', *American Journal of Botany,* 98: 1148-63.
Goertz, G. P. et al. (2019). 'Mosquito small RNA responses to West Nile and insect-specific virus infections in *Aedes* and *Culex* mosquito cells', *Viruses,* 11: 271.
Gorbalenya, A. E. et al. (2002). 'The palm subdomain-based active site is internally permuted in viral RNA-dependent RNA polymerases of an ancient lineage', *Journal of Molecular Biology,* 324: 47-62.
Grabherr, M. G. et al. (2011). 'Full-length transcriptome assembly from RNA-Seq data without a reference genome', *Nature Biotechnology,* 29: 644-U130.
Grybchuk, D. et al. (2018). 'Viral discovery and diversity in trypanosomatid protozoa with a focus on relatives of the human parasite *Leishmania*', *Proceedings of the National Academy of Sciences of the United States of America,* 115: E506-E515.
Herrero, N., Marquez, S. S. and Zabalgogeazcoa, I. (2009). 'Mycoviruses are common among different species of endophytic fungi of grasses', *Archives of Virology,* 154: 327-30.
Hillman, B. I. and Cai, G. (2013). 'The family Narnaviridae: Simplest of RNA viruses', *Advances in Virus Research, Vol 86: Mycoviruses,* 86: 149-76.
Hollings, M. (1962). 'Viruses associated with a die-back disease of cultivated mushroom', *Nature,* 196: 962-65.
Holmes, E. C. and Duchene, S. (2019). 'Can sequence phylogenies safely infer the origin of the global virome?', *Mbio,* 10: e00289-19.
Hrabáková, L., Koloniuk, I. and Petrzik, K. (2017). *'Phomopsis longicolla* RNA virus 1-Novel virus at the edge of myco- and plant viruses', *Virology,* 506: 14-8.
Huttinga, H., Wichers, H. and Dieleman-Van Zaayen, A. (1975). 'Filamentous and polyhedral virus-like particles in *Boletus edulis*', *Netherlands Journal of Plant Pathology,* 81: 102-6.
Jacob-Wilk, D., Turina, M. and Van Alfen, N. K. (2006). 'Mycovirus cryphonectria hypovirus 1 elements cofractionate with trans-golgi network membranes of the fungal host *Cryphonectria parasitica'*, *Journal of Virology,* 80: 6588-96.
James, J. D., Saunders, G. C. and Owens, S. J. (1998). 'Isolation and partial characterisation of double-stranded RNA-containing viruses of orchid mycorrhizal fungi', *Springer Lab Manual Series; Mycorrhiza manual*: 425-36.
Kadowaki, K. and Halvorson, H. O. (1971). ' Appearance of a new species of ribonucleic acid during sporulation in *Saccharomyces cerevisiae* ', *Journal of Bacteriology,* 105: 826-30.
Kaefer, S. et al. (2019). 'Re-assessing the diversity of negative strand RNA viruses in insects', *Plos Pathogens,* 15: e1008224.
Kalyaanamoorthy, S. et al. (2017). 'ModelFinder: fast model selection for accurate phylogenetic estimates', *Nature Methods,* 14: 587-9.

Kanhayuwa, L. et al. (2015). 'A novel mycovirus from *Aspergillus fumigatus* contains four unique dsRNAs as its genome and is infectious as dsRNA', *Proceedings of the National Academy of Sciences of the United States of America,* 112: 9100-5.
Kohler, A. et al. (2015). 'Convergent losses of decay mechanisms and rapid turnover of symbiosis genes in mycorrhizal mutualists', *Nature Genetics,* 47: 410-U176.
Koonin, E. V. (1991). 'The phylogeny of RNA-dependent RNA polymerases of positive-strand RNA viruses', *Journal of General Virology,* 72: 2197-206.
Koonin, E. V. et al. (2020). 'Global organization and proposed megataxonomy of the virus world', *Microbiology and molecular biology reviews,* 84: e00061-19.
Krupovic, M., Dolja, V. V. and Koonin, E. V. (2020) 'The LUCA and its complex virome', *Nature Reviews Microbiology*. https://doi.org/10.1038/s41579-020-0408-x
Krupovic, M., Dolja, V. V. and Koonin, E. V. (2019). 'Origin of viruses: primordial replicators recruiting capsids from hosts', *Nature Reviews Microbiology,* 17: 449-58.
Lacourt, I. et al. (2000). 'Genetic polymorphism and metal sensitivity of *Oidiodendron maius* strains isolated from polluted soil', *Annals of Microbiology,* 50: 157-66.
Langmead, B. and Salzberg, S. L. (2012). 'Fast gapped-read alignment with Bowtie 2', *Nature Methods,* 9: 357-U354.
Li, C.-X. et al. (2015). 'Unprecedented genomic diversity of RNA viruses in arthropods reveals the ancestry of negative-sense RNA viruses', *Elife,* 4: e05378.
Li, H. et al. (2009). 'The sequence alignment/map format and SAMtools', *Bioinformatics,* 25: 2078-9.
Lin, Y. et al. (2020). 'A novel narnavirus from the plant-pathogenic fungus *Magnaporthe oryzae*', *Archives of Virology,* 165: 1235-40.
Liu, L. et al. (2014). 'Fungal negative-stranded RNA virus that is related to bornaviruses and nyaviruses', *Proceedings of the National Academy of Sciences of the United States of America,* 111: 12205-10.
Márquez, L. M. et al. (2007). 'A virus in a fungus in a plant: Three-way symbiosis required for thermal tolerance', *Science,* 315: 513-515.
Martino, E. et al. (2018). 'Comparative genomics and transcriptomics depict ericoid mycorrhizal fungi as versatile saprotrophs and plant mutualists', *New Phytologist,* 217: 1213-29.
Martino, E. et al. (2003). 'Solubilization of insoluble inorganic zinc co mpounds by ericoid mycorrhizal fungi derived from heavy metal polluted sites', *Soil Biology & Biochemistry,* 35: 133-41.
Martino, E. et al. (2000). 'Ericoid mycorrhizal fungi from heavy metal polluted soils: their identification and growth in the presence of zinc ions', *Mycological Research,* 104: 338-44.
Marzano, S.-Y. L. et al. (2016). 'Identification of diverse mycoviruses through metatranscriptomics characterization of the viromes of five major fungal plant pathogens ', *Journal of Virology,* 90: 6846-63.
Mascia, T. et al. (2019). 'Infection of *Colletotrichum acutatum* and *Phytophthora infestans* by taxonomically different plant viruses', *European Journal of Plant Pathology,* 153: 1001-17.
Milne, I. et al. (2016). 'Tablet: visualizing next-generation sequence assemblies and mappings', *Plant Bioinformatics.* Springer: 253-68.
Mollentze, N. and Streicker, D. G. (2020). 'Viral zoonotic risk is homogenous among taxonomic orders of mammalian and avian reservoir hosts', *Proceedings of the National Academy of Sciences of the United States of America,* 117: 9423-30.
Nerva, L. et al. (2016). 'Multiple approaches for the detection and characterization of viral and plasmid symbionts from a collection of marine fungi', *Virus Research,* 219: 22-38.
Nerva, L. et al. (2017). 'Mycoviruses of an endophytic fungus can replicate in plant cells: evolutionary implications', *Scientific Reports,* 7: 1908.

Nerva, L. et al. (2019a). 'Isolation, molecular characterization and virome analysis of culturable wood fungal endophytes in esca symptomatic and asymptomatic grapevine plants', *Environmental Microbiology,* 21: 2886-904.
Nerva, L. et al. (2019b). 'The mycovirome of a fungal collection from the sea cucumber *Holothuria polii*', *Virus Research,* 273: 197737.
Ong, J. W. L. et al. (2016). 'Novel Endorna-like viruses, including three with two open reading frames, challenge the membership criteria and taxonomy of the *Endornaviridae*', *Virology,* 499: 203-11.
Ong, J. W. L. et al. (2017). 'The challenges of using high-throughput sequencing to track multiple bipartite mycoviruses of wild orchid-fungus partnerships over consecutive years', *Virology,* 510: 297-304.
Ong, J. W. L. et al. (2018). 'Novel and divergent viruses associated with Australian orchid-fungus symbioses', *Virus Research,* 244: 276-83.
Osaki, H. et al. (2016). 'Multiple virus infection in a single strain of *Fusarium poae* shown by deep sequencing', *Virus Genes,* 52: 835-47.
Pearson, M. N. et al. (2009). 'Mycoviruses of filamentous fungi and their relevance to plant pathology', *Molecular Plant Pathology,* 10: 115-28.
Pearson, V. and Read, D. J. (1973). 'The biology of mycorrhiza in the Ericaceae. I. The isolation of the endophyte and synthesis of mycorrhizas in aseptic culture', *New Phytologist,* 72: 371-9.
Perez, M., Craven, R. C. and de la Torre, J. C. (2003). 'The small RING finger protein Z drives arenavirus budding: Implications for antiviral strategies', *Proceedings of the National Academy of Sciences of the United States of America,* 100: 12978-83.
Perotto, S. et al. (1996). 'Molecular diversity of fungi from ericoid mycorrhizal roots', *Molecular Ecology,* 5: 123-31.
Petrzik, K. et al. (2016). 'Molecular characterization of a new monopartite dsRNA mycovirus from mycorrhizal *Thelephora terrestris* (Ehrh.) and its detection in soil oribatid mites (Acari: Oribatida)', *Virology,* 489: 12-19.
R Development Core Team, R. (2011). 'R: A language and environment for statistical computing', R foundation for statistical computing Vienna, Austria.
Rastgou, M. et al. (2009). 'Molecular characterization of the plant virus genus *Ourmiavirus* and evidence of inter-kingdom reassortment of viral genome segments as its possible route of origin', *Journal of General Virology,* 90: 2525-35.
Read, D. J. (1974). '*Pezizella ericae* sp.nov., the perfect state of a typical mycorrhizal endophyte of Ericaceae', *Transactions of the British Mycological Society*, 63: 381-3.
Read, D. J. and Stribley, D. P. (1973). 'Effect of mycorrhizal infection on nitrogen and phosphorus nutrition of ericaceous plants', *Nature-New Biology,* 244: 81-2.
Richaud, A. et al. (2019). 'Vertical transmission in *Caenorhabditis* nematodes of RNA molecules encoding a viral RNA-dependent RNA polymerase', *Proceedings of the National Academy of Sciences of the United States of America,* 116: 24738-47.
Rodriguez, R. J. et al. (2009). 'Fungal endophytes: diversity and functional roles', *New Phytologist,* 182: 314-30.
Rohwer, F., Prangishvili, D. and Lindell, D. (2009). 'Roles of viruses in the environment', *Environmental Microbiology,* 11: 2771-4.
Roossinck, M. J. (2019). 'Evolutionary and ecological links between plant and fungal viruses', *New Phytologist,* 221: 86-92.
Ryan, F. (2009). *Virolution,* London: Collins.
Sato, Y. et al. (2020). 'Hadaka Virus 1: a capsidless eleven-segmented positive-sense single-stranded RNA virus from a phytopathogenic fungus, *Fusarium oxysporum*', *mBio,* 11.
Shi, M. et al. (2016). 'Redefining the invertebrate RNA virosphere', *Nature,* 540: 539-43.

Sievers, F. et al. (2011). 'Fast, scalable generation of high-quality protein multiple sequence alignments using Clustal Omega', *Molecular Systems Biology,* 7.
Smith, S. E. and Read, D. J. (2008). *Mycorrhizal Symbiosis*, 3rd Edition. New York: Academic Press.
Steitz, T. A. (1998). 'Structural biology - A mechanism for all polymerases', *Nature,* 391: 231-232.
Stielow, B. and Menzel, W. (2010). 'Complete nucleotide sequence of TaV1, a novel totivirus isolated from a black truffle ascocarp (*Tuber aestivum* Vittad.)', *Archives of Virology,* 155: 2075-8.
Suttle, C. A. (2007). 'Marine viruses - major players in the global ecosystem', *Nature Reviews Microbiology,* 5: 801-12.
Takahashi, H. et al. (2019). 'Virus latency and the impact on plants', *Frontiers in Microbiology,* 10: 2764.
te Velthuis, A. J. W. (2014). 'Common and unique features of viral RNA-dependent polymerases', *Cellular and Molecular Life Sciences,* 71: 4403-20.
Trifinopoulos, J. et al. (2016). 'W-IQ-TREE: a fast online phylogenetic tool for maximum likelihood analysis', *Nucleic Acids Research,* 44: W232-5.
Turina, M., Prodi, A. and Van Alfen, N. K. (2003). 'Role of the Mf1-1 pheromone precursor gene of the filamentous ascomycete *Cryphonectria parasitica*', *Fungal Genetics and Biology,* 40: 242-51.
Vainio, E. J. et al. (2015). 'Diagnosis and discovery of fungal viruses using deep sequencing of small RNAs', *Journal of General Virology,* 96: 714-25.
Vainio, E. J. et al. (2017). 'Occurrence of similar mycoviruses in pathogenic, saprotrophic and mycorrhizal fungi inhabiting the same forest stand', *FEMS microbiology ecology,* 93.
Vallino, M. et al. (2011). 'Specific regions in the Sod1 locus of the ericoid mycorrhizal fungus *Oidiodendron maius* from metal-enriched soils show a different sequence polymorphism', *Fems Microbiology Ecology,* 75: 321-31.
Waldron, F. M., Stone, G. N. and Obbard, D. J. (2018). 'Metagenomic sequencing suggests a diversity of RNA interference-like responses to viruses across multicellular eukaryotes', *Plos Genetics,* 14: e1007533.
Weiss, M. et al. (2016). 'Sebacinales - one thousand and one interactions with land plants', *New Phytologist,* 211: 20-40.
Wesolowski, M. and Wickner, R. B. (1984). 'Two new double-stranded RNA molecules showing non-mendelian inheritance and heat inducibility in *Saccharomyces cerevisiae*', *Molecular and Cellular Biology*, 4: 181-7.
Wolf, Y. I. et al. (2018). 'Origins and evolution of the global RNA virome', *Mbio,* 9: e02329-18.
Wu, F. et al. (2020). 'A new coronavirus associated with human respiratory disease in China', *Nature,* 579: 265–9.
Yu, X. et al. (2010). 'A geminivirus-related DNA mycovirus that confers hypovirulence to a plant pathogenic fungus', *Proceedings of the National Academy of Sciences of the United States of America,* 107: 8387-92.
Zoll, J., Verweij, P. E. and Melchers, W. J. G. (2018). 'Discovery and characterization of novel *Aspergillus fumigatus* mycoviruses', *Plos One,* 13: e0200511.

Figure legends and Tables

Figure 1. Main features of contigs related to members of *Lenarviricota* from ERM and ORM fungi. A: Schematic representation of genome organization, with the main features. RdRP=RNA-dependent RNA polymerase; ORF=open reading frame; nt=nucleotides; A-sd, B-sd, C-sd and D-sd are, respectively the A, B, C and D subdomains of the RdRP palm domain. B: Phylogenetic tree derived from alignments of the most closely related putative RdRP amino acid sequences inside the *Lenarviricota* clade. Model of substitution: Blosum62+F+I+G4. Consensus tree is constructed from 1000 bootstrap trees. Log-likelihood of consensus tree: -49081.578022. At nodes, the percentage bootstrap values. The main existing and proposed taxonomic clades (class and family for the five smaller parentheses, phylum for the large one) are grouped with parenthesis. C: TAE 1.5% agarose gel of qPCR products to show that there is no DNA template corresponding to transcripts of Oidiodendron maius splipalmivirus 1 RNA1 and RNA2 (OmSPV1 RNA1 and OmSPV1 RNA2). As a control for amplification we included a fragment of the *O. maius* actin gene. Lanes are labeled with the template used for the qPCR reaction and include an infected *O. maius* isolate (E27) and an uninfected isolate (E34). D: 5' and 3' untranslated region of the sequence alignment of OmSPV1 RNA1 and OmSPV1 RNA2 genomic fragments.

Figure 2. Northern blot analysis of narna-like contigs DN37559 and DN43802 representing the two genome segments of the Oidiodendron maius splipalmivirus 1 (OmSPV1). A: Schematic representation of the position of the run-off transcript probes with codes identifying their orientation. In black, sense-oriented transcripts that hybridize with minus sense anti-genomic RNA intermediate. In red, antisense-oriented transcripts that hybridize with plus sense genomic RNA. **B:** Top panels, autoradiography exposed 2 hrs with samples of total RNA (circa 3 ug/gel lane). The RNAs in the panel on the far left were hybridized first with probe #4 and subsequently with a tomato brown rugose fruit probe (ToBRFV-S1) that can can be used as standard for RNA size (6.3 Kb for the genomic RNA and 0.7 kb for subgenomic RNA2). Lower panel is a methylene blue stained membrane to show different ribosomal RNA loadings (rRNA). Sample nomenclatures include E27 as the infected *O. maius* isolate and isolates O4 and E34 as negative controls. Mock is RNA extracted from a mock inoculated tomato plant. A blue arrow in this panel points to the position of the OmSP1 genomic RNAs, whereas black arrows points to the genomic and subgenomic RNA2 of ToBRFV.

Figure 3. Protein alignments of contigs DN37559 and DN43802 representing the two genome segments of the Oidiodendron maius splipalmivirus 1 (OmSPV1). A: Five protein sequences retrieved from different previously published assemblies from fungal RNAseq projects with some homology to OmSPV1 RNA1. Only the carboxy terminal of the proteins is shown. **B**: Proteins from the same libraries with homology to OmSPV1 RNA2 ORF encoded protein. Only the amino terminal of the protein alignment is displayed. OmSPV1 RNA1 is marked with a red asterisk and OmSPV1 RNA2 is marked with a blue asterisk. In the alignment, eight conserved regions already characterized for viral RdRPs could be observed and are marked with red rectangles for OmSPV1 RNA1 -related viruses and blue rectangles for OmSPV1 RNA2 -related sequences. Conserved regions are named I to VIII following Koonin et al. (Koonin 1991); regions IV, V, VI and VII are linked to motifs A, B, C and D from the RdRP palm subdomain, respectively. 20074 is the code for the fungal isolate MUT4935 isolated from *Posidonia oceanica*. F2 and F4

are libraries from mixed fungal isolates from esca-infected grapevines, and Holo3 is a library that comprises a number of fungal isolates from *Holothuria polii*.

Figure 4. Main features of the Tulasnella bunyavirales-like virus 1 (TuBlV1). A: The genome organization of TuBlV1 with the main genomic features (ORFs and domains). Black bi-directional arrows indicate the position of RT-PCR amplification products to cover the whole genome. Unidirectional black and red arrows represent the position and orientation of the run-off transcripts used as probes in Northern blot analysis. Nc=Nucleocapsid; RdRP=RNA-dependent RNA polymerase; ORF=open reading frame; nt=nucleotide. **B**: Maximum likelihood phylogenetic tree derived from RdRP alignment of TuBlV1 with a number of bunyavirales representative of the main families in the order, (and two rhabdovirus used as outgroup). Amino acid substitution model is VT+F+I+G4. Log-likelihood of the tree: -200570.9602. Bootstrap values in percentage are displayed at each node. The tree is unrooted.

Figure 5. Evidence of a contiguous 12 kb genomic segment for Tulasnella bunyavirales-like virus 1 (TuBlV1). A: Overlapping RT-PCR of segments spanning the whole TuBlV1 genome. Lanes 1 to 6 correspond to segments A, B, F, C, D and E of Figure 4. M is the 1 kb Ladder. The three stronger bands correspond to 1 kb, 3 kb and 7 kb, respectively. **B:** Northern blot analysis of total RNA extracts from ORM fungal isolates O4 and O7 positive for Ceratobasidium ambivirus 1 (CeAmV1) and for TuBlV1, respectively. Specific probes for each of the two viruses were hybridized in succession, in order to derive the specificity of each probe. Here the result after the second hybridization is displayed, which therefore shows all the bands hybridizing with both probes. Red arrows point to the two bands specific for the ambivirus. Dotted black arrows point to the position of cross reactivity with ribosomal RNA. The black arrow points at the position of the TuBlV1 virus-specific RNA bands; upper panels are autoradiography exposed for 7 days. Lower panel is ribosomal RNA stained with methylene blue (the membrane picture was stretched vertically). Probes used are specified in Fig. 4 and Fig. 8; rRNA=ribosomal RNA.

Figure 6. Genome organization of ambiviruses and their putative RdRP palm subdomains. A: Schematic representation of the genome organization of Tulasnella ambivirus 1 and Tulasnella ambivirus 2 (TuAmV1 and TuAmV2). Open reading frames (ORF) are represented by green (ORFB) and orange (ORFA) arrows. **B:** Alignment of conserved motifs of canonical viral RNA-dependent RNA polymerases (RdRPs) and ORFA proteins of ambiviruses. RdRPs were retrieved from alignment by Gorbalenya et al. (2002) and aligned using Clustal Omega. Conserved domains A, B and C were selected from the alignment and sequences were aligned again on Clustal adding the ORFA sequences of ambiviruses discovered in the present study. Results were displayed on MEGA6. Canonical motifs are surrounded by the red rectangles with conserved residues marked by the red arrows. The putative motifs and conserved amino acids of ambiviruses surrounded by the black squares and black arrows indicate conserved residues. The sequences used for the alignment are as follows: tobacco vein mottling virus (TVMV, 8247947); feline calicivirus F9 (FCVF9, 130538); infectious flacherie virus (InFV, 3025415); Drosophila C virus (DCV, 2388673); human poliovirus type 3 Leon strain (PV3L, 130503); rice tungro spherical virus (RTSV, 9627951); cowpea severe mosaic virus (CPSMV, 549316); Tulasnella ambivirus 1 (TuAmV1, MN793991); Tulasnella ambivirus 2 (TuAmV2, MN793992); Tulasnella ambivirus 5

(TuAmV5, MN793996); Tulasnella ambivirus 3 (TuAmV3, MN793994); Ceratobasidium ambivirus 1 (CeAmV1, MN793993); and Tulasnella ambivirus 4 (TuAmV4, MN793994).

Figure 7. Northern blot analysis of total RNA extracted from ORM fungal strains harboring ambiviruses. A: ORM fungal strains O4, O7 and O10, of which the latter was infected by Tulasnella ambivirus 1 (TuAmV1). The probes used for TuAmV1 are presented at the bottom of each panel. Film was exposed to the membrane for 24 hrs. The blue arrow points to the position of the single specific band hybridizing with the probe. Dotted black arrows point to unspecific hybridization to ribosomal RNAs (rRNAs). **B:** ORM fungal strains O4 and O7 of which the former hosts Ceratobasidium ambivirus 1 (CeAmV1). Film was exposed to the membrane for 12 hrs. The left end panel was hybridized first with probe B2 and subsequently with a tomato brown rugose fruit virus probe (ToBRFV-S1) that can be used as standard for RNA size (6.3 Kb for the genomic RNA and 0.7 kb for subgenomic RNA2). In this panel a black arrow points to the position of ToBRFV genomic RNA and subgenomic RNA2, a blue arrow to the putative CeAmV1 genomic RNA and the red arrow to the position of the putative CeAmV1 dimer. Dotted black arrows point to the position of cross hybridizing rRNA. In both A and B, lower panels are methylene blue stained membranes rRNA loadings. Mock is RNA extracted from a mock inoculated tomato plant. At the top of each panel is a schematic representation of the position of the run-off transcript probes with codes that identify their orientation. In black, sense-oriented transcripts that hybridize with minus sense anti-genomic RNA intermediate. In red, antisense-oriented transcripts that hybridize with plus sense genomic RNA.

Table 1. Viral contigs found in our collection of ericoid and orchid mycorrhizal fungi. The main features of each virus contig are reported together with the suggested virus names. The first hit in our viral database BLAST search is also reported, with the main features of the alignment.

GenBank ID	Virus name	Domain[a]	Length	Contig[b]	Accession[c]	Name[c]	Per. Ident.[c]	Query cov[c]	E-value[c]	Mapping reads[d]
MN736964	Oidiodendron maius splipalmivirus 1 RNA1	N/A	2455	DN37559_c1_g1_i3	QIR30299.1	Plasmopara viticola associated narnavirus 20	48.519	86%	0	231825
MN736965	Oidiodendron maius splipalmivirus 1 RNA2	N/A	2481	DN43802_c0_g4_i1	APG76982.1	Beihai narna-like virus 22	26.37	23%	0.089	194000
MN736966	Oidiodendron maius ourmia-like virus 1	RdRP	2087	DN47822_c2_g3_i2	QAB47442.1	Combu positive-strand RNA mycovirus	60.741	77%	0	749959
MN736968	Ceratobasidium mitovirus 1	RdRP	4501	DN39198_c0_g3_i1	AWY10986.1	Sclerotinia sclerotiorum mitovirus 28	50.435	14%	2.24E-56	143938
MN738550	Ceratobasidium endornavirus 1	RdRP	21599	DN44545_c0_g1_i1	YP_009552276.1	Rhizoctonia solani endornavirus 1	40.344	72%	0	17370
MN738551	Ceratobasidium endornavirus 2	RdRP	18941	DN44360_c0_g1_i1	QDW65431.1	Rhizoctonia solani endornavirus 4	33.979	70%	0	~20000
MN738552	Tulasnella barnavirus 1	RdRP	4389	DN27349_c0_g2_i1	ALD89112.1	Rhizoctonia solani barnavirus 1	52.688	31%	3.70E-156	17296
MN793991	Tulasnella ambivirus 1	N/A	4724	DN30310_c0_g1_i1	AQM32755.1	hypothetical protein [Agaricus bisporus]	28.08	8%	0.051	5172
MN793992	Tulasnella ambivirus 2	N/A	4777	DN33730_c1_g1_i1	AQM32755.1	hypothetical protein [Agaricus bisporus]	31.46	5%	0.065	1662
MN793993	Ceratobasidium ambivirus 1	N/A	4915	DN43545_c0_g4_i1	AQM32755.1	hypothetical protein [Agaricus bisporus]	29.88	19%	4.00E-19	51 000
MN793994	Tulasnella ambivirus 3	N/A	5120	DN37145_c0_g1_i6	AQM32755.1	hypothetical protein [Agaricus bisporus]	30.35	17%	1.00E-24	1074
MN793995	Tulasnella ambivirus 4	N/A	4924	DN32762_c1_g1_i1	AQM32755.1	hypothetical protein [Agaricus bisporus]	30.49	19%	3.00E-22	620
MN793996	Tulasnella ambivirus 5	N/A	4632	DN36360_c0_g1_i2	AQM32754.1	hypothetical protein [Agaricus bisporus]	29.81	39%	2.00E-74	736
MN793997	Tulasnella bunyavirales-like virus 1	RdRP	12157	DN37204_c0_g2_i1	APG79361.1	Hubei orthoptera virus 2	26.891	5%	4.75E-07	13972

[a] Domains were searched using Motif Search at https://www.genome.jp/tools/motif/ using both Pfam and NCBI-CDD databases
[b] The code is that provided automatically by Trinity software after assembly. The suffixes in the contig IDs were removed in the text for simplicity.
[c] All the parameters refer to the first hit in BlastX searches of nr NCBI databases.
[d] Total number of reads present in each library mapping to each of the putative viral contigs assembled by Trinity software

Table 2. Number of reads, in the four RNA libraries, mapping the positive and negative orientation of virus segments and control host genes (underlined).

		1-ENDO			2-ENDO			XEO			ORM		
Contig	Length	All	Negative	Positive	All	Negative	Positive	All	Negative	Positive	All	Negative	Positive
***O. maius* Actin**	1743	2338	**7**	**1162**	NA	NA	NA	NA	NA	NA	NA	NA	NA
***O. maius* Tubulin**	2526	21434	**151**	**10566**	NA	NA	NA	NA	NA	NA	NA	NA	NA
***O. maius* ATPase**	3691	48570	**55**	**24230**	NA	NA	NA	NA	NA	NA	NA	NA	NA
***Tulasnella* Actin**	1409	NA	NA	NA	NA	NA	NA	3506	**0**	**1753**	NA	NA	NA
DN37559_c1_g1_i3[a]	2455	203672	**91605**	**10231**	0	0	0	340738	**154367**	**16002**	NA	NA	NA
DN43802_c0_g4_i1[a]	2481	347830	**159583**	**14332**	2	1	0	620664	**285480**	**24852**	NA	NA	NA
DN47822_c2_g3_i2[a]	2087	642822	**473**	**320938**	783912	**264**	**391692**	2	0	1	NA	NA	NA
TuBlV1[b]	12157	NA	NA	NA	NA	NA	NA	NA	NA	NA	13972	**3734**	**3252**
TuBlV1-Nc[b]	780	NA	NA	NA	NA	NA	NA	NA	NA	NA	938	**46**	**423**
TuBlV1-ORF3[b]	3410	NA	NA	NA	NA	NA	NA	NA	NA	NA	4130	**1566**	**499**
TuBlV1-RdRP[b]	7523	NA	NA	NA	NA	NA	NA	NA	NA	NA	7092	**1738**	**1808**

[a] DN37559_c1_g1_i3=Oidiodendron maius splipalmivirus 1 RNA1; DN43802_c0_g4_i1=Oidiodendron maius splipalmivirus 1 RNA2; DN47822_c2_g3_i2=Oidiodendron maius ourmia-like virus contig 1
[b] TuBlV1=Tulasnella bunyavirales-like virus 1. Nc=nucleocapsid; RdRP=RNA-dependent RNA polymerase

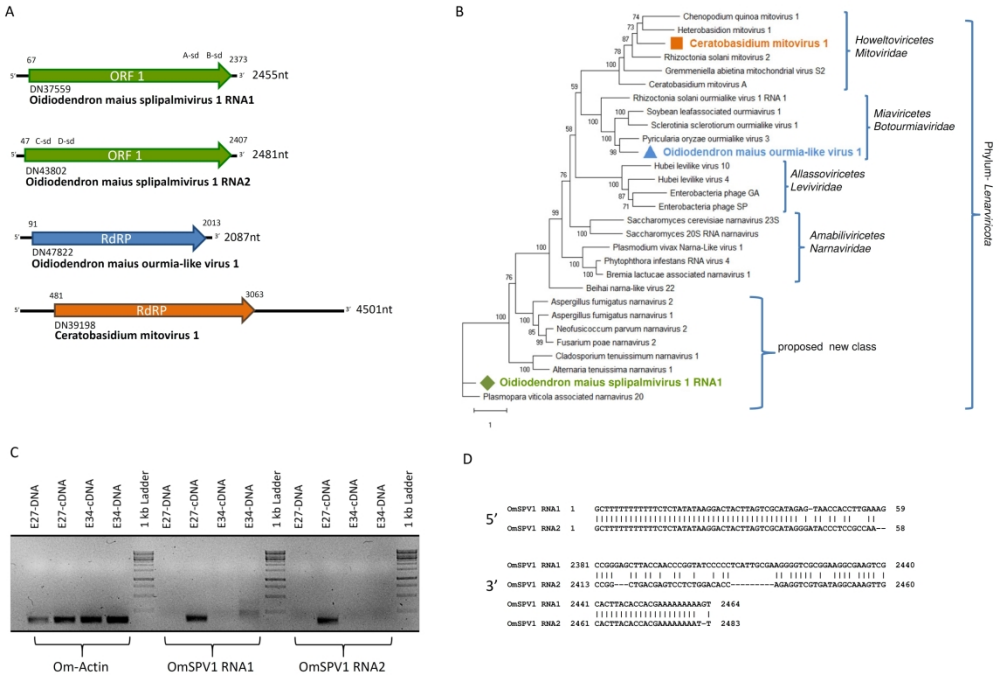

Figure 1. Main features of contigs related to members of *Lenarviricota* from ERM and ORM fungi. A: Schematic representation of genome organization, with the main features. RdRP=RNA-dependent RNA polymerase; ORF=open reading frame; nt=nucleotides; A-sd, B-sd, C-sd and D-sd are, respectively the A, B, C and D subdomains of the RdRP palm domain. B: Phylogenetic tree derived from alignments of the most closely related putative RdRP amino acid sequences inside the *Lenarviricota* clade. Model of substitution: Blosum62+F+I+G4. Consensus tree is constructed from 1000 bootstrap trees. Log-likelihood of consensus tree: -49081.578022. At nodes, the percentage bootstrap values. The main existing and proposed taxonomic clades (class and family for the five smaller parentheses, phylum for the large one) are grouped with parenthesis. C: TAE 1.5% agarose gel of qPCR products to show that there is no DNA template corresponding to transcripts of Oidiodendron maius splipalmivirus 1 RNA1 and RNA2 (OmSPV1 RNA1 and OmSPV1 RNA2). As a control for amplification we included a fragment of the *O. maius* actin gene. Lanes are labeled with the template used for the qPCR reaction and include an infected *O. maius* isolate (E27) and an uninfected isolate (E34). D: 5' and 3' untranslated region of the sequence alignment of OmSPV1 RNA1 and OmSPV1 RNA2 genomic fragments.

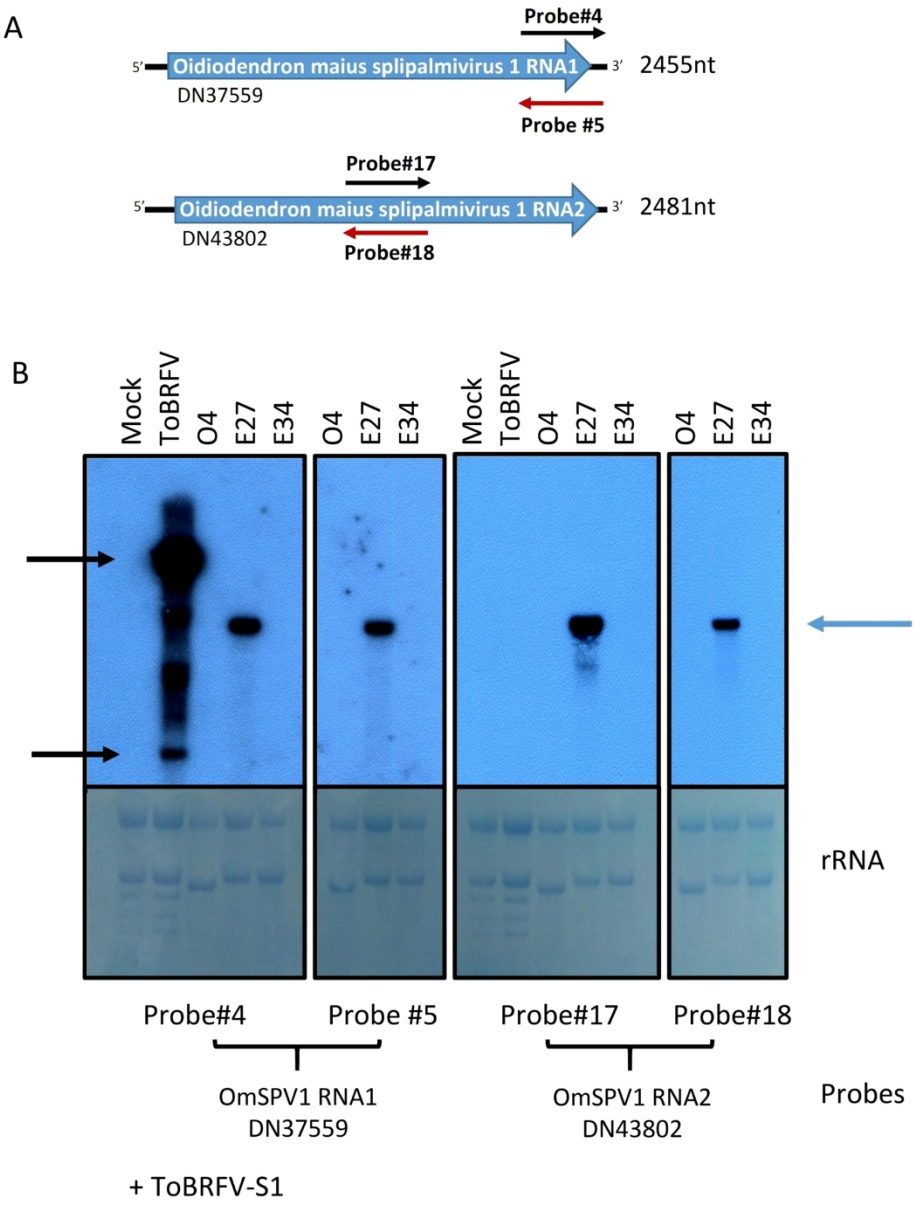

Figure 2. Northern blot analysis of narna-like contigs DN37559 and DN43802 representing the two genome segments of the Oidiodendron maius splipalmivirus 1 (OmSPV1). A: Schematic representation of the position of the run-off transcript probes with codes identifying their orientation. In black, sense-oriented transcripts that hybridize with minus sense anti-genomic RNA intermediate. In red, antisense-oriented transcripts that hybridize with plus sense genomic RNA. B: Top panels, autoradiography exposed 2 hrs with samples of total RNA (circa 3 ug/gel lane). The RNAs in the panel on the far left were hybridized first with probe #4 and subsequently with a tomato brown rugose fruit probe (ToBRFV-S1) that can can be used as standard for RNA size (6.3 Kb for the genomic RNA and 0.7 kb for subgenomic RNA2). Lower panel is a methylene blue stained membrane to show different ribosomal RNA loadings (rRNA). Sample nomenclatures include E27 as the infected *O. maius* isolate and isolates O4 and E34 as negative controls. Mock is RNA extracted from a mock inoculated tomato plant. A blue arrow in this panel points to the position of the OmSP1 genomic RNAs, whereas black arrows points to the genomic and subgenomic RNA2 of ToBRFV.

99x130mm (600 x 600 DPI)

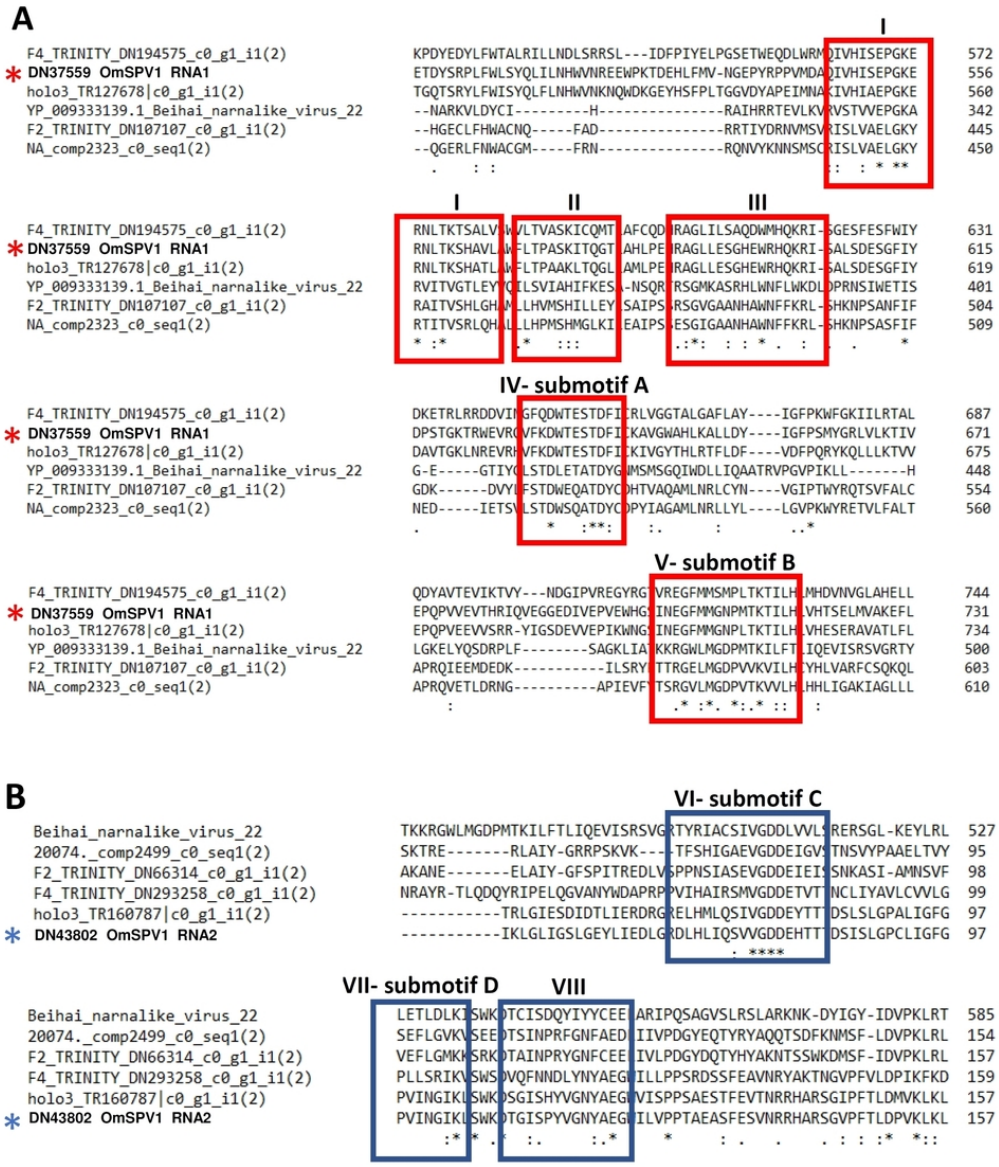

Figure 3. Protein alignments of contigs DN37559 and DN43802 representing the two genome segments of the Oidiodendron maius splipalmivirus 1 (OmSPV1). A: Five protein sequences retrieved from different previously published assemblies from fungal RNAseq projects with some homology to OmSPV1 RNA1. Only the carboxy terminal of the proteins is shown. B: Proteins from the same libraries with homology to OmSPV1 RNA2 ORF encoded protein. Only the amino terminal of the protein alignment is displayed. OmSPV1 RNA1 is marked with a red asterisk and OmSPV1 RNA2 is marked with a blue asterisk. In the alignment, eight conserved regions already characterized for viral RdRPs could be observed and are marked with red rectangles for OmSPV1 RNA1 -related viruses and blue rectangles for OmSPV1 RNA2 -related sequences. Conserved regions are named I to VIII following Koonin et al. (Koonin 1991); regions IV, V, VI and VII are linked to motifs A, B, C and D from the RdRP palm subdomain, respectively. 20074 is the code for the fungal isolate MUT4935 isolated from *Posidonia oceanica*. F2 and F4 are libraries from mixed fungal isolates from esca-infected grapevines, and Holo3 is a library that comprises a number of fungal isolates from *Holothuria polii*.

80x93mm (300 x 300 DPI)

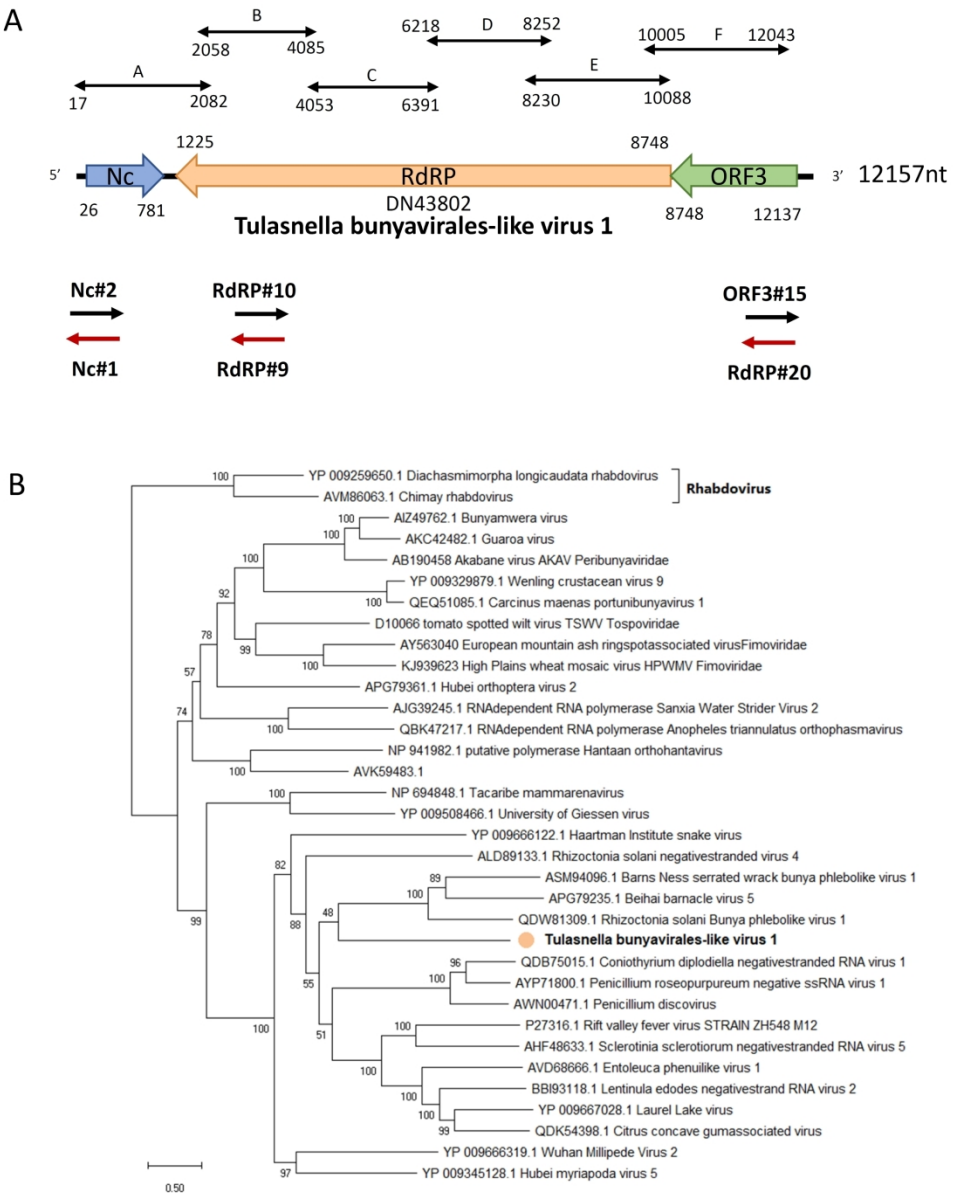

Figure 4. Main features of the Tulasnella bunyavirales-like virus 1 (TuBlV1). A: The genome organization of TuBlV1 with the main genomic features (ORFs and domains). Black bi-directional arrows indicate the position of RT-PCR amplification products to cover the whole genome. Unidirectional black and red arrows represent the position and orientation of the run-off transcripts used as probes in Northern blot analysis. Nc=Nucleocapsid; RdRP=RNA-dependent RNA polymerase; ORF=open reading frame; nt=nucleotide. B: Maximum likelihood phylogenetic tree derived from RdRP alignment of TuBlV1 with a number of bunyavirales representative of the main families in the order, (and two rhabdovirus used as outgroup). Amino acid substitution model is VT+F+I+G4. Log-likelihood of the tree: -200570.9602. Bootstrap values in percentage are displayed at each node. The tree is unrooted.

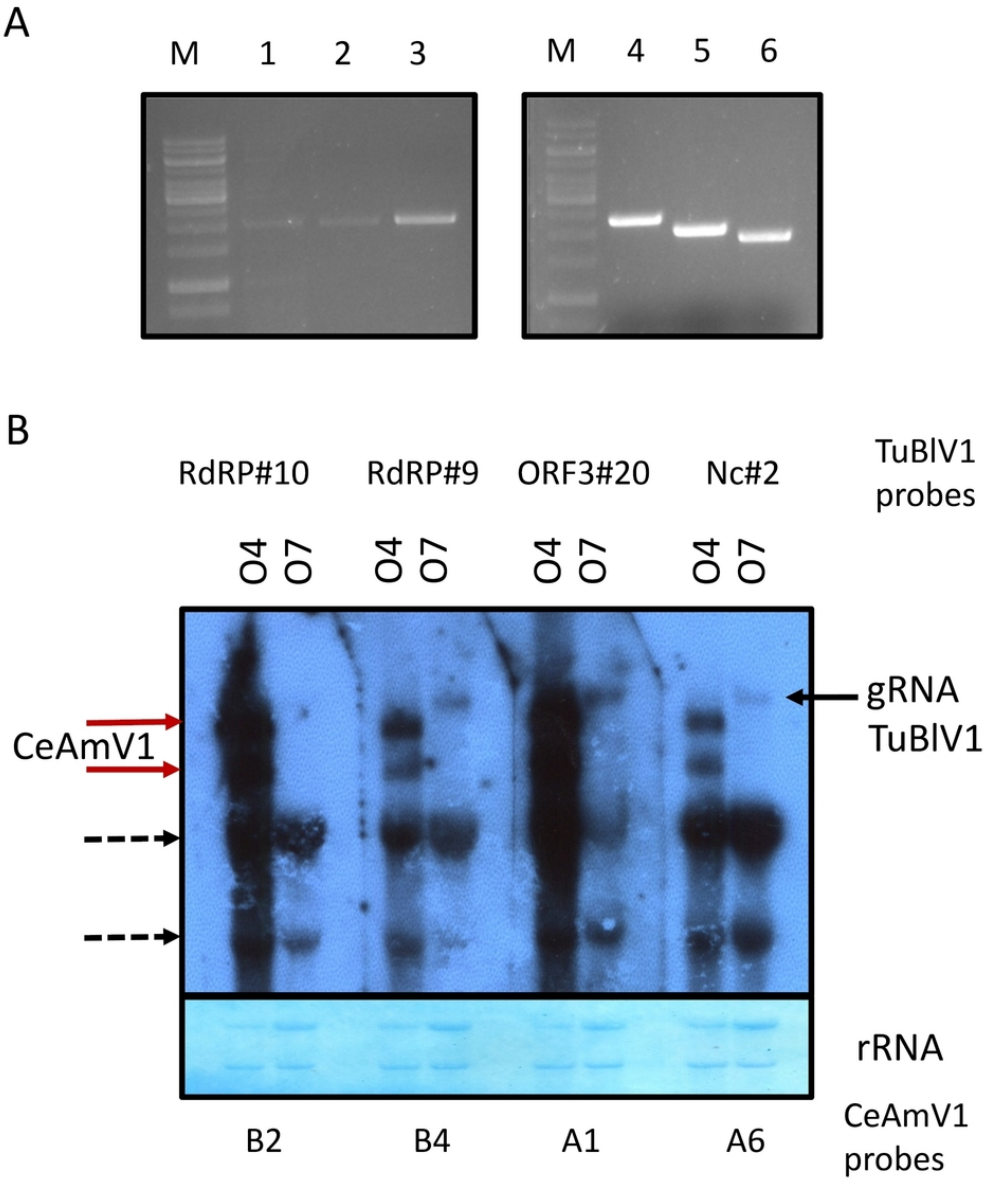

Figure 5. Evidence of a contiguous 12 kb genomic segment for Tulasnella bunyavirales-like virus 1 (TuBlV1). A: Overlapping RT-PCR of segments spanning the whole TuBlV1 genome. Lanes 1 to 6 correspond to segments A, B, F, C, D and E of Figure 4. M is the 1 kb Ladder. The three stronger bands correspond to 1 kb, 3 kb and 7 kb, respectively. B: Northern blot analysis of total RNA extracts from ORM fungal isolates O4 and O7 positive for Ceratobasidium ambivirus 1 (CeAmV1) and for TuBlV1, respectively. Specific probes for each of the two viruses were hybridized in succession, in order to derive the specificity of each probe. Here the result after the second hybridization is displayed, which therefore shows all the bands hybridizing with both probes. Red arrows point to the two bands specific for the ambivirus. Dotted black arrows point to the position of cross reactivity with ribosomal RNA. The black arrow points at the position of the TuBlV1 virus-specific RNA bands; upper panels are autoradiography exposed for 7 days. Lower panel is ribosomal RNA stained with methylene blue (the membrane picture was stretched vertically). Probes used are specified in Fig. 4 and Fig. 8; rRNA=ribosomal RNA.

80x94mm (300 x 300 DPI)

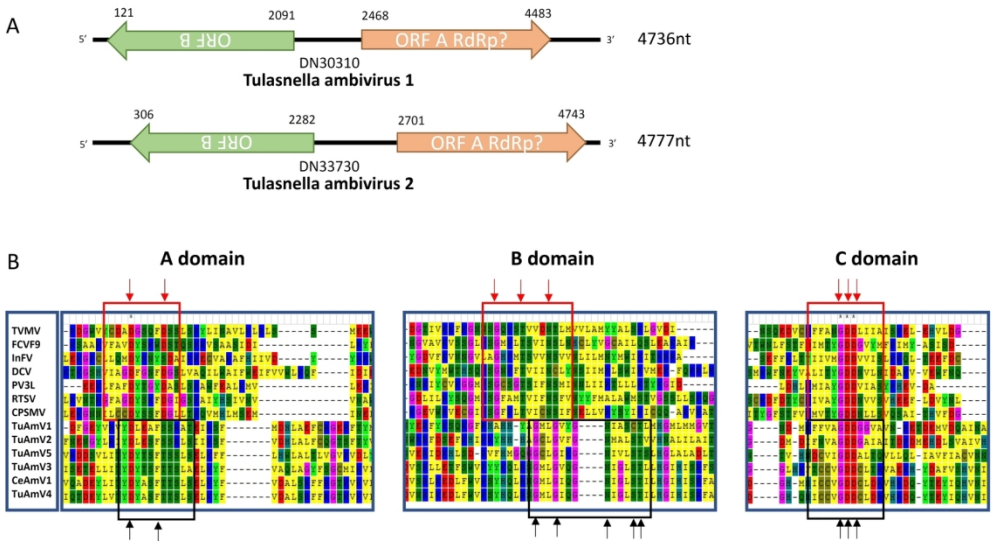

Figure 6. Genome organization of ambiviruses and their putative RdRP palm subdomains. A: Schematic representation of the genome organization of Tulasnella ambivirus 1 and Tulasnella ambivirus 2 (TuAmV1 and TuAmV2). Open reading frames (ORF) are represented by green (ORFB) and orange (ORFA) arrows. B: Alignment of conserved motifs of canonical viral RNA-dependent RNA polymerases (RdRPs) and ORFA proteins of ambiviruses. RdRPs were retrieved from alignment by Gorbalenya et al. (2002) and aligned using Clustal Omega. Conserved domains A, B and C were selected from the alignment and sequences were aligned again on Clustal adding the ORFA sequences of ambiviruses discovered in the present study. Results were displayed on MEGA6. Canonical motifs are surrounded by the red rectangles with conserved residues marked by the red arrows. The putative motifs and conserved amino acids of ambiviruses surrounded by the black squares and black arrows indicate conserved residues. The sequences used for the alignment are as follows: tobacco vein mottling virus (TVMV, 8247947); feline calicivirus F9 (FCVF9, 130538); infectious flacherie virus (InFV, 3025415); Drosophila C virus (DCV, 2388673); human poliovirus type 3 Leon strain (PV3L, 130503); rice tungro spherical virus (RTSV, 9627951); cowpea severe mosaic virus (CPSMV, 549316); Tulasnella ambivirus 1 (TuAmV1, MN793991); Tulasnella ambivirus 2 (TuAmV2, MN793992); Tulasnella ambivirus 5 (TuAmV5, MN793996); Tulasnella ambivirus 3 (TuAmV3, MN793994); Ceratobasidium ambivirus 1 (CeAmV1, MN793993); and Tulasnella ambivirus 4 (TuAmV4, MN793994).

149x80mm (300 x 300 DPI)

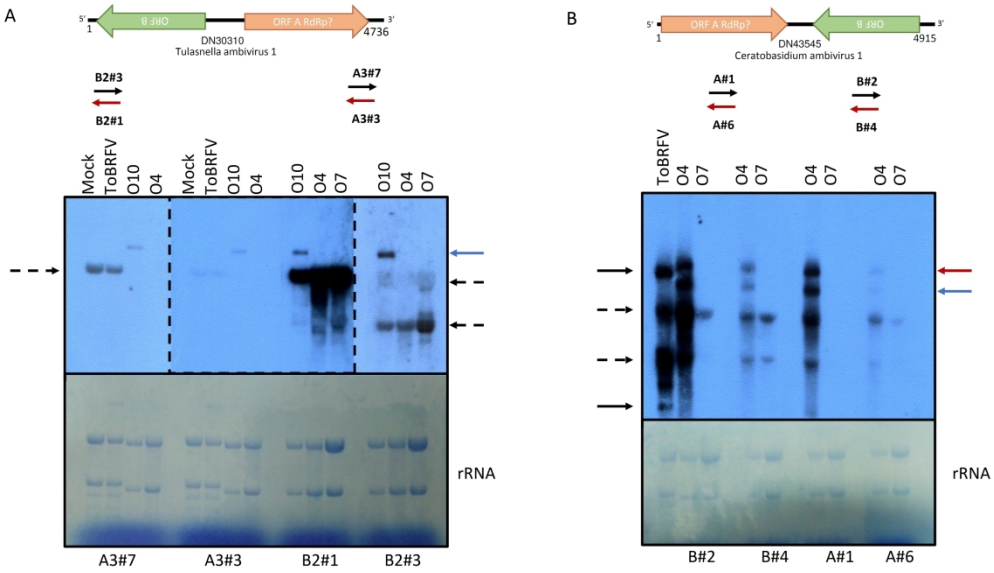

Figure 7. Northern blot analysis of total RNA extracted from ORM fungal strains harboring ambiviruses. A: ORM fungal strains O4, O7 and O10, of which the latter was infected by Tulasnella ambivirus 1 (TuAmV1). The probes used for TuAmV1 are presented at the bottom of each panel. Film was exposed to the membrane for 24 hrs. The blue arrow points to the position of the single specific band hybridizing with the probe. Dotted black arrows point to unspecific hybridization to ribosomal RNAs (rRNAs). B: ORM fungal strains O4 and O7 of which the former hosts Ceratobasidium ambivirus 1 (CeAmV1). Film was exposed to the membrane for 12 hrs. The left end panel was hybridized first with probe B2 and subsequently with a tomato brown rugose fruit virus probe (ToBRFV-S1) that can be used as standard for RNA size (6.3 Kb for the genomic RNA and 0.7 kb for subgenomic RNA2). In this panel a black arrow points to the position of ToBRFV genomic RNA and subgenomic RNA2, a blue arrow to the putative CeAmV1 genomic RNA and the red arrow to the position of the putative CeAmV1 dimer. Dotted black arrows point to the position of cross hybridizing rRNA. In both A and B, lower panels are methylene blue stained membranes rRNA loadings. Mock is RNA extracted from a mock inoculated tomato plant. At the top of each panel is a schematic representation of the position of the run-off transcript probes with codes that identify their orientation. In black, sense-oriented transcripts that hybridize with minus sense anti-genomic RNA intermediate. In red, antisense-oriented transcripts that hybridize with plus sense genomic RNA.